ASSESSING THE IMPACT OF URBAN EXPANSION ON LAND SURFACE TEMPERATURE USING GEOGRAPHICAL INFORMATION SYSTEMS AND REMOTE SENSING TECHNIQUES:A CASE STUDY OF DUHOK-IRAQ

DABAN KADHIM OMAR DABBAGH

MASTER᾿S THESIS

DEPARTMENT OF BIOENGINEERING AND SCIENCES

KAHRAMANMARAS - TURKEY 2015

T.R.

KAHRAMANMARAS SUTCU IMAM UNIVERSITY

GRADUATE SCHOOL OF NATURAL AND APPLIED SCIENCES

ASSESSING THE IMPACT OF URBAN EXPANSION ON LAND SURFACE TEMPERATURE USING GEOGRAPHICAL INFORMATION SYSTEMS AND REMOTE SENSING TECHNIQUES:A CASE STUDY OF DUHOK-IRAQ

DABAN KADHIM OMAR DABBAGH

Thesis submitted in candidature for

the degree of Master in

Department of Bioengineering and Sciences

KAHRAMANMARAS -TURKEY 2015

M.Sc. thesis entitled "Assessing the Impact of Urban Expansion on Land Surface Temperature Using Geographical Information Systems and Remote Sensing Techniques : A Case Study of Duhok-IRAQ." and prepared by Daban Kadhim Omar DABBAGH, who is a student at Bioengineering and Sciences Department, Institute of Science And Technology, Kahramanmaras Sutcu Imam University,03/06/2015 was certified by all the/majority jury members, whose signatures are given below.

Assist. Prof. Hakan OĞUZ (Supervisor)   ....……………………..

Department of Landscape Architecture

Kahramanmaras Sutcu İmam University

Assoc. Prof. Murat KARABULUT (Member)   ....……………………..

Department of Geography

Kahramanmaras Sutcu Imam University

Assoc. Prof. Hasan SERIN (Member)   ....……………………..

Department of Forest Industry Engineering

Kahramanmaras Sutcu Imam University

I approve that the above signatures related to the members.

Assoc. Prof. Mustafa ŞEKKELİ   ....……………………..

Director of Graduate School of Natural and Applied Science

Kahramanmaras Sutcu Imam University

DECLARATION

I hereby declare that all information in the thesis has been obtained and presented in accordance with academic rules and ethical conduct. I also declare that, as required by these rules and conduct, I have fully cited and referenced all material and results that are not original to this work.

Daban Kadhim Omar DABBAGH

Note: the original and other sources used in this thesis, the declaration, tables, figures and photographs showing the use of resources, subject to the provisions of Law No. 5846 on Intellectual and Artistic Works.

ŞEHRİN GENİŞLEMESİNİN ARAZİ YÜZEYİ ISISI ÜZERİNDEKİ ETKİLERİNİN COĞRAFİ BİLGİ SİSTEMLERİ VE UZAKTAN SENSÖR TEKNİKLERİ İLE DEĞERLENDİRİLMESİ: IRAK, DUHOK'TA VAKA ÇALIŞMASI
(YÜKSEK LİSANS TEZİ)

DABAN KADHIM OMAR DABBAGH

ÖZET

Bu araştırma Erbil Şehrindeki şehrin genişlemesinin tespiti ve değerlendirilmesi ile bunun 1998 ila 2011 yılları arasında LST üzerindeki etkilerinin değerlendirilmesi için GIS verileri ile entegreolanLandsat-5 TM görüntü veri kaydı ile tekniklerinin kullanılmasıyla gerçekleştirilmiştir. Çalışmamızın amacı Duhok Şehri ilçeleri ve çevre alanlarına uzamsal dağılımı değerlendirmek ve analiz etmek olup LST ile diğer farklı arazi örtüsü türleri arasındaki ilişkinin de araştırılmasını içermektedir. Bu çalışmamız farklı arazi örtüsü türlerinin sınıflandırılmasında ve arazi örtüsü sınıfları açısından değişikliklerin tespiti için denetimli bir sınıflandırma uygulanmıştır. Daha sonra çalışma sahası için LST elde edilmesi için bölünmüş pencere algoritmasından yararlanılmıştır. Sonuçlar kentsel arazi örtüsü anlamında geniş ve hızlı bir yayılmanın bu bölgede gerçekleştiğini göstermektedir. Bu 1998'de %5.98 iken 2011 yılında %17.62'ye yükselmiştir. Buna ilaveten 1998 ila 2011 yılları arasında yoğun bitki örtüsü artışı olmuş bu da sırası ile %31.69 ve %14.54 oranlarına sahiptir. Ayrıca, uzamsal LST dağılımı şehir ilçelerinde eşit ve eş merkezli gerçekleşmemiştir. Şehir çevresinde yeni yapılanan ilçeler eskiden kurulu bulunan ilçelere nazaran en yüksek LST düzeyini göstermiş ancak her iki yıllarda da en sıcak yüzeye sahip bölümler şehir dışındaki alanlarda yoğunlaşmıştır. Ayrıca araştırma uzamsal LST dağılımının çeşitli olduğunu ve arazi örtüsü sınıflarında farklılık gösterdiğini ortaya koymuştur. En düşük LST su ve yoğun bitki örtüsü sınıfta görülürken su kütlesi 25ºCve 28ºCsıcaklıkta ve yoğun bitki örtüsü bulunan yerlerde sırasıyla 1998 ve 2011 yıllarında 30ºCve 32ºC ölçülmüştür. Bunun aksine en yüksek LST (diğer sınıflar) 1998 ve 2011 yıllarında sırasıyla - 39 ºCve 42 ºC olmuştur. Sonuç olarak bu araştırma Duhok şehrindeki su kütlesi ile yeşil alanların yüzeylerin soğutulması ve hava sıcaklığının düşürülmesi sürecinde güçlü bir rol oynadığını ortaya oymuş ve LST ile NDVI arasındaki korelasyon analizlerinden bu açıkça görülmüştür ve bu da her iki yıllarda da güçlü negatif bir ortalama ortaya koymuştur. Özellikle sırası ile 1998 ve 2011 yıllarında bu değer -0.86ve -0.82olmuştur.

Sonuç olarak uzak sensör cihazlarının kullanımı ve sonuçların GIS verileri ve teknikleri ile entegre edilmesi geliştirme süreçleri ve Duhok Şehri için gelecekteki yerel ve bölgesel planlama açısından faydalı bir etki sağlayan en efektif araç olduğu bulunmuştur.

Anahtar kelimeler: Arazi kullanımı/arazi örtüsü, LST, Termal kuşak, Landsat, GIS, RS.

ASSESSING THE IMPACT OF URBAN EXPANSION ON LAND SURFACE TEMPERATURE USING GEOGRAPHICAL INFORMATION SYSTEMS AND REMOTE SENSING TECHNIQUES: A CASE STUDY OF DUHOK-IRAQ (M.Sc. THESIS)

DABAN KADHIM OMAR DABBAGH

ABSTRACT

This research is an investigation using Landsat-5 TM imagery data integrated with GIS data and techniques in order to detect and evaluate the urban expansion of Erbil City, and its impact on LST between the years 1998 and 2011. The purpose of this study is to evaluate and analyze the spatial distribution of LST based on the Duhok City districts and surrounding areas, involving an investigation of the relationship between LST and different land cover types. In this study a supervised classification was used to classify different land cover types, and to detect any changes in terms of the land cover classes. Then, a Radiative Transfer Equation (RTE) was utilized to retrieve LST for the study area.

The results indicate that a vast and fast expansion has taken place in this area in terms of urban land cover. This increased from 5.98% in 1998 to 17.62% in 2011. In addition, dense vegetation decreased noticeably between the years 1998 and 2011, which was 31.69 % and 14.54% respectively. Furthermore, the results of the spatial distribution of LST regarding the city districts were non-equal and non-concentric. The newly built districts around the city recorded the highest LST compared with the older constructed districts, hence the hottest surface places were concentrated in areas outside the city for both years. Furthermore, this research revealed that the spatial distribution of LST was various, due of the variation in land cover classes. As the lowest LST was recorded in the water and dense vegetation class, when the water body was 25ºC and 28ºC and dense vegetation was 30ºC and 32ºC in 1998 and 2011 respectively. In contrast, the highest LST was recorded in (Other classes) - 39 ºC and 42 ºC 'in 1998 and 2011 respectively. As a result, this research determined that the water body and green areas in Duhok City have a powerful role to play in the process of cooling surfaces and lowering air temperatures, as is clearly shown from the results of the correlation analysis between LST and NDVI, which revealed a strong negative average for both years. Specifically this was -0.86 and -0.82 for 1998 and 2011 respectively.

In conclusion, the utilization of remote sensing devices and integrating the results with GIS data and techniques was found to be the most effective tool in terms of having a utilitarian impact on development processes and local and regional planning for Duhok City in the future.

Key words: Land use/land cover, LST, Thermal band, Landsat, GIS, RS.

University of Kahramanmaras Sutcu Imam

Graduate School of Natural and Applied Sciences

Department of Bioengineering and Sciences, June / 2015

Supervisor: Assist. Prof. Hakan OĞUZ

Page number: 61

ACKNOWLEDGEMENTS

TABLE OF CONTENTS

LIST OF FIGURES

LIST OF TABLES

LIST OF SYMBOLS AND ABBREVIATIONS

DN   :Digital Numbers

GCM   :Global circulation models

GIS   :Geographical Information System

Ha   :Hectare

LST   :Land Surface Temperature

LU/LC   :Land Use/Land Cover

NDVI   :Normalized Different Vegetation Index

RS   :Remote Sensing

RTE   :Radiative Transfer Equation

TC   :Tasselled Cap

TM   :Thematic Mapper

TOA   :Top-of-atmosphere

UHI   :Urban Heat Island

USGS   :United States Geological Survey

UTM   :Universal Transverse Mercator Coordinate System

WGS   :World Geodetic System

1. INTRODUCTION

Urban expansion has recently become a "hot topic" which has attracted a great deal of attention in the academic and scientific world. According to the Cambridge Dictionary, the words "expansion" or "sprawl" mean to "…cover a large area of land with buildings which have been added at different time so that it looks untidy". Moreover, the expansion of urban areas is commonly recognized as a way of creating an unacceptable environment in terms of air quality and lack of natural resource management. This is because urban sprawl changes natural land cover into man-made land cover in order to serve human needs. This also involves converting arable land into built-up land (Mallick *et al.*, 2008). In other words, the process of urbanization brings variations in the physical characteristics of ground surface components like the thermal capacity of the land surface, surface albedo and the amount of moisture in the soil. This brings about changes in the natural environment in urban and surrounding suburban areas. Thus, urbanization interferes negatively with the natural environment and has a direct or indirect impact on human mortality, human health and activities, and on the quality of life in the urban environment (Bhatta, 2010; Gartland, 2008; Saleh, 2011).

Urban environment mainly under impact of urbanization as a result of population spread, and changes in the physical properties and chemical concentration of the atmosphere by the uses of human in urban area. The cumulative effect of all these is referred to as urban heat island effects, simply defined as a man-made area which is clearly warmer than the surrounding countryside. It is usually measured by the term 'urban heat island intensity', which is defined as the difference between the maximum urban temperature and the background rural temperature (Oke, 1988). This phenomenon was first investigated by Luke Howard (Mills, 2007) whose research on the climate of London represented the beginning of the field in the 1810s. A heat island exists because the land surface in urban areas absorbs heat from the variety of sources such as from the sun and from the other man made materials like factors and so on. This is coupled with concentrated energy consumption and less ventilation than in rural areas. As a result, a 'warm island' is formed in a 'cool sea'. The difference in temperature is commonly bigger at night comparing with the day time, stronger with weak winds and most noticeable during summer and winter.

In general there are two kinds of heat island: (1) Atmospheric Urban Heat Island – forms in the air and is measured by weather stations and mobile transverses. (2) Surface Urban Heat Island - forms at the surface and is measured by remote sensing. The adverse effects of an Urban Heat Island (UHI) are significant. It deteriorates the quality of the living environment around us, rises of energy consumption, raises emissions of air pollutants and greenhouse gases, impairs water quality, and even increases mortality rates (Akbari et al., 2008; Rizwan et al., 2008). Due to adverse environmental and economic impacts on society, heat island determination and mitigation research increasingly draws the attention of urban climate researchers and engineers. The assessment of UHIs varies in terms of research approaches and applied measurement techniques (Arnfield, 2003; Grimmond, 2005; Rizwan et al., 2008). The types of built-up areas and building materials used differ significantly in terms of thermal and optical properties. Thus, this study is mainly focused on the impact of built-up types on UHIs by investigating the distribution of urban land surface temperatures across built-up structure types in a city.

It appears from the definition of UHIs and the factors which lead to UHIs emerging, that the land surface temperature (LST) has the distinctive characteristic of participating in the process of creating UHIs. As Voogt and Oke (2003) state "LST modulates the air temperature of the lowest types of urban atmosphere". Thus, LST plays an important role in studies of UHIs and environmental changes. LST has an obvious impact on certain atmospheric and environmental issues such as the process of upward terrestrial radiation and control of the sensible surface and latent heat flux exchanges within the atmosphere (Prigent *et al*., 2003). Therefore, LST is an essential key variable in studies of regional and global climate change, and in estimating the surface energy balance (Jin and Dickinson, 1999; Oluesyi *et al*., 2011; Sun and Pinker, 2003). In addition, LST plays an important role in the physics of land-surface processes. It is a significant means of obtaining information about the physical properties of different land surface types. So, as Kerr *et al*. (2005) and Wan and Dozier (1996) emphasize, the estimation of LST is necessary for a variety of climatic, geological, hydrological, vegetation monitoring, and global circulation models (GCM), including GCM studies and applications. In fact, researchers studying the retrieval or estimation of LST are currently in the process of exploring and measuring how hot to the touch land surface can become. Many years ago, LST was identified as a type of air surface temperature which can usually be measured by local meteorological stations. However, LST is totally different from air surface

temperature. For instance, the process of heating and cooling a land surface happens more quickly than the same processes with regard to air surface temperature. Thus, LST refers to the land's surface skin temperature. As a result, the process of heating the land surface is a complex one which has a strong relationship with other factors such as surface emissivity, the moisture of the soil, roughness and solar radiation.

For all of these reasons, many national and international organizations associated with a number of scientific sectors have nowadays begun to pay attention to the urgent need for collecting and monitoring information about LST at national and international levels. For instance, the Intergovernmental Panel on Climate Change (IPCC, 2001) referred to the urgent need to use remote sensing data in terms of LST for studying global warming due to the limitations of the World Metrological Organization which prevent it from carrying out such sensing.

Remotely sensed thermal infrared (TIR) data have contributed to addressing the problem caused by UHIs through the estimation of LST. A number of satellite and airborne sensors, such as Landsat TM/ETM+, AVHRR, MODIS, ASTER and TIMS have provided thermal infrared (TIR) data of the Earth's surface. These TIR data have been widely used to retrieve LST. In addition to LST, these TIR sensors may also be used to get emissivity for various land cover types with (Mitraka *et al*., 2012). LST is a main factor in determining surface radiation and energy exchange. The spatial distribution of LST is governed by surface heat fluxes that are clearly affected by urbanization (Qin, Li, Gao & Zhang, 2006; Sun & Yu, 2013).

For this reason, an LST-related study was conducted regarding urban expansion in the city of Duhok in the north of Iraq. This was carried out because the rapid and vast expansion of Duhok had been well documented in the literature and other non-scientific sources. However, the impact of urban expansion on LST has remained a largely un-researched area, especially with the use of remote sensing and techniques. Also, in the two last decades, this region and the city in particular have faced serious environmental problems such as drought, desertification and recurring sand storms during the hot months of the year.

Thus, this study represents important research that has had a utilitarian impact on development processes and on local and regional planning with regard to Duhok City. Using new techniques such as remote sensing, it is very important to detect and monitor

environmental changes, which can help to speed up decision processes about the problems which the human environment may face in terms of urban areas. Such research may also help to understand the reasons for the changes involved. In addition, it is a way to help public and urban planners understand the characteristics of the distribution of LST, and may help to find ways of improving situations in which LST poses a problem.

2.LITERATURE REVIEW

According to some studies, which have used satellite thermal bands to retrieve land surface temperatures (LST) related to urban climates. A Landsat thermal band is one of the most widely-used means of collecting data in this field. For this reason, in this section of the literature review, we will attempt to review only the most relevant work in the sense of ones that have used Landsat imagery to retrieve LST.

It appears from the reviewed studies that a large number of these studies focused on the association between different the cover of land classes and LST. It was due to the different thermal characteristics of the different land covers surveyed, in that they produced differences in terms of LST. For instance, Honjo *et al*. (2004) focused on the impact of green spaces on LST in the case of Tokyo, Japan. The traditional classification method with Landsat-5 TM and ETM+7 was used to identify and recognize different land covers within the study area. They used shape, size, and areas of green space as criteria for evaluating the role of green areas with regard to LST. Therefore, this study found that the shape and size of green areas in Tokyo had a significant role in reducing overall LST .A similar study was done by Rajeshware and Mani (2014) who used Landsat-8 thermal bands to evaluate the impact of vegetation on the LST of the Dindigul District, Tamil Nadu, India. In this study, a split window algorithm was used to retrieve LST. For this purpose, they used NDVI to estimate emissivity over the study area. As in the previous study, the outcome revealed that the highest LST was found over barren land, and the lowest LST was noted over vegetated land cover.

Kwarteng and Small (2005) compared two cities in two different geographical locations. The first was Kuwait City, located in the Arabian desert area, and the second was New York City. They used Landsat ETM+ and the satellite brightness temperature equation to retrieve LST. The results underlined clearly that, in Kuwait City, LST was lower than in the surrounding desert areas owing to the lack of significant amounts of vegetation in the surrounding areas. Consequently, almost all the land cover in the surrounding areas delivered higher solar radiation than in the urban setting due to the lack of a process of evaporation which leads to changing the heat to humidity. In contrast, in New York City, the LST was higher in built-up areas than in surrounding areas as a result of the density of the vegetation which circled the city, and which played a part in cooling the air through the process of evaporating the received solar radiation. In other words, this

study's results showed that geographical conditions help the process of recording low LST in cities areas rather than in surrounding ones. For instance, because Kuwait City is situated in a dry and desert area, LST was lower inside the city than in the surrounding areas.

A similar study has been done by Frey *et al*. (2005). They selected two coastal cities in the United Arab Emirates (Dubai and Abu Dhabi). Both cities are located in a dry desert environment. In general, the main aim of this investigation was to investigate the role of urban areas in a dry environment in terms of producing a Urban Cool Island (UCI). The results clearly indicate that both cities produced a daily UCI due to the albedo around each city with regard to dry land, which was higher than in the urban areas. This led to high surface temperatures in the former.

Habib (2007) used Landsat-5 TM to retrieve LST in the Saudi Arabian city of Dammam. The results of this study produced two significant points. Firstly, it was found that well-planned urban areas led to LST being controlled and reduced. For example, as widely documented in the literature, the Central Business District (CBD), which was the core of the city, was supposed to have a high LST. However, Damma's CBD recorded a lower LST than the surrounding districts as a result of having a large amount of greenery which helped to decrease LST compared to other parts of the city. This study's second point recommended encouraging people to continue to construct buildings in the desert at the same time as using sufficient amounts of green space to decrease LST.

Furthermore, the role of evaporation in the process of the spatial distribution of LST has been studied. This was done by Ahmed *et al*. (200**5**) in the Gezira region of Sudan's desert. They used the SEBAL algorithm to calculate evaporation. This study found that evaporation was an important parameter in reducing LST in this area. The following results supported this point. In 2001, the ratio of evaporation was 4.36% over the vegetated areas, with a 300.7 K degree of LST. However, on barren land, in the same year, the LST was 313.6 K with a 0.0 ratio of evaporation. This had an obvious impact in terms of vegetation reducing LST by producing evaporation. In addition, Bounoua *et al*. (2009) used Landsat ETM+ data to identify the impact of LST on the dynamics of cycling water, and the balance of carbon and surface energy in the semi-arid region of the urbanized area of Oran City in Algeria. The results demonstrated that it was possible for an urban area to play a positive role in decreasing LST in arid and semi-arid areas. As revealed by this study, the urban expansion of Oran City had a weak impact in terms of producing an island

of heat in this region. In addition, the results showed that the dynamics of these indicators were affected greatly by the kind of covering of land and the identified vegetation. The most significant indicator was the reduction of LST and carbon uptake. As a result, this study recommended the continuing process of constructing buildings in this region, along with planting and growing trees, which were quite important in reducing LST and providing a better environment for the people living in this city**.**

Zhang and Ban (2011) used Landsat TM to study Beijing's LST. They attempted to investigate the impact of urban expansion on LST between the years 2004 and 2009. NDVI was used as a parameter to extract surface emissivity. They found a non-equal and non-concentric spatial pattern distribution of LST among the city districts. In other words, LST in Beijing's city varied between districts, since some recorded high LST and others recorded low LST. However, all of these districts were inside the city and not in the suburban areas. These obvious differences between the districts were related to green spaces and thermal characteristics. In addition, this study employed a correlation analysis between NDVI and LST, for the years 2004 and 2009. The results were a negative correlation of -0.751 and -0.732, respectively. Similarly, Salah (2011) studied Baghdad, the capital city of Iraq. He focused on the impact of the expansion of Baghdad City on LST between the years 1961 and 2001. A traditional classification method was used based on high resolution IKONOS data. The study area divided into seven different classes. A traditional simple equation was used to convert satellite digital numbers to satellite brightness temperatures. This study pointed out that the LST increased between the identified years due to the alteration of vegetation land cover relate to man-made land cover. For example, in the orchard area, the LST was about 33.37ºC. However, on barren lands and built up areas, it was about 46.97ºC and 49.01ºC respectively. Consequently, this study revealed that the expansion of Baghdad City caused a reduction in vegetation cover and caused LST to increase, especially in those areas which had no vegetation.

Likewise, in the Indian city of Vijayawada, Kumar et al. (2012) studied the impact of different land cover types on LST. Landsat ETM+ was used as the primary data, and the researchers used satellite brightness temperatures retrieved from the thermal band. In addition, NDVI was used for two purposes: firstly, to identify the impact of vegetation on LST; and secondly, to retrieve land surface emissivity based on NDVI values. The results demonstrated that the correlation between NDVI and LST was about (-0.79). Furthermore, with regard to this study's results, it appears that the areas of greenery had a powerful role

to play in controlling and reducing LST in that they found the highest LST to be recorded on built-up land (320 K) and the lowest LST recorded in areas of greenery (about 299 K).

Far from investigating and finding the relationship between land cover and LST, Oluseyi *et al.* (2011) used Landsat data to identify the reasons for mosquito infestation in Anyigba, Nigeria. The aim of this study was to help people in this area overcome the problem which they faced from mosquitoes transferring disease. For this reason, two Landsat images were used for 1995 and 2006. In general, the researchers looked for changes in using of lands and land cover, and the influence on LST. As a result, they were able to identify the hottest places in the city and relate this information to mosquito infestation. The results demonstrated that change in covering of land and land use induced changes in LST and, as a result, those areas that recorded high LST on built-up land were infested with mosquitoes. Clearly, the opposite was seen with low LST in the bodies of land covered by greenery and water.

In addition, Oguz (2013) attempted to build a computer-based program to calculate LST in a simple and quick way compared with other approaches. He prepared a program based on C++ using a single-channel algorithm to retrieve LST using Landsat thermal bands. It's important to say that this approach is one of the most accurate methods for calculating LST. This is due to the use of a number of variables in the process of calculating LST.

To sum up, it can be deduced that there were some common objectives among the literature, which were used widely and employed in the study of LST in urban areas. These objectives were such as the impact of urban areas on LST, the relationship of LST and different types of land cover; and the role of vegetation, and so on. In addition, a great number of pieces of literature stated the same results regarding urban areas and LST. They found that LST was higher over urban areas than the surrounding areas. In contrast, as shown in the works by Ahmed *et al.*(2005), Bounoua *et al.* (2009),Habib (2007), Kwarten and Small (2005) some of the literature revealed an opposite result. They stated that, within urban areas, LST was slightly lower or lower than suburban areas owing to the geographical and climatic condition of these areas, located in desert or semi-arid regions. Furthermore, there was a sort of agreement across the literature about the role of areas of greenery in controlling and reducing LST.

Therefore, through the investigations described in different milestone papers about LST using remote sensing data and its associated techniques, it can be deduced that there were some common objectives within the literature, which were used widely and were employed in the study of land surface temperature using Landsat data. However, this study clearly identified two pronounced research gaps within the literature. These gaps are (i) the differences within the literature were in terms of the techniques that were used for retrieving LST. For this reason, this study has attempted to close this gap by using the most accurate method to calculate LST based on Landsat Thermal band. The method works on various parameters which help to calculate LST in proper way. (ii) As stated clearly in the literature, there was a specific thermal characteristic for each type of land cover. However, it seems that there were almost no studies about the spatial distribution of LST within urban areas and surrounding areas. For this reason, this study attempts to investigate the spatial distribution of LST in Duhok city and its surrounding area, and has concentrated on the connection between LST and different type of land cover, especially with regard to vegetation and built-up land. This was done by employing the Radiative Transfer Equation (RTE) with a Landsat-5 TM thermal band, as well as integrating with a geographical information system (a spatial analysis tool).

3. MATERIAL AND METHODS

3.1.Study Area

The study field is located in the Duhok city center, which is located in the northwest of Iraq . As it is shown in the figure (3.1). In addition, Duhok is an important and strategic city. In the last three decades, the city has continuously developed economically, and it has expanded in areas. According to the land use classification data for the years 1998 and 2011, the area of urbanization in 1998 was 22.8 square kms On the other hand, this area increased to 50.9 square km - a percentage increase of 55.3%. This rate is very high given the short period of time.

The city of Duhok is the field of study. It has an oval shape. It is located in a narrow valley between two parallel mountains, and two rivers pass through the field of study. One of them is called the Duhok River while the second is a seasonal river called the Hishkaro River. They join together in the southwest near the Kavarki district.

The field of study is located between latitudes (36° 54' 19", 36° 48' 33") and longitudes (42° 53' 12", 43° 05' 39"); at (413-1003M) above sea level. According to latest census (2009), the total population of the studied area was (308302).

Regarding the status of the climate of the field of study, its climate according to the classification (koppen) is in the class CSA which recognizes with characteristics continental semi dry and round. The system's rain pattern is the same system as the one found in the Mediterranean Sea.

According to the climatic data recorded at the city of Duhok's climate station for the years 1998 and 2011, the average air temperature in the field of study is 19.8ºC and 21.3 ºC for the years 1998 and 2011 respectively. This indicates that both air temperature averages are quite close to each other.
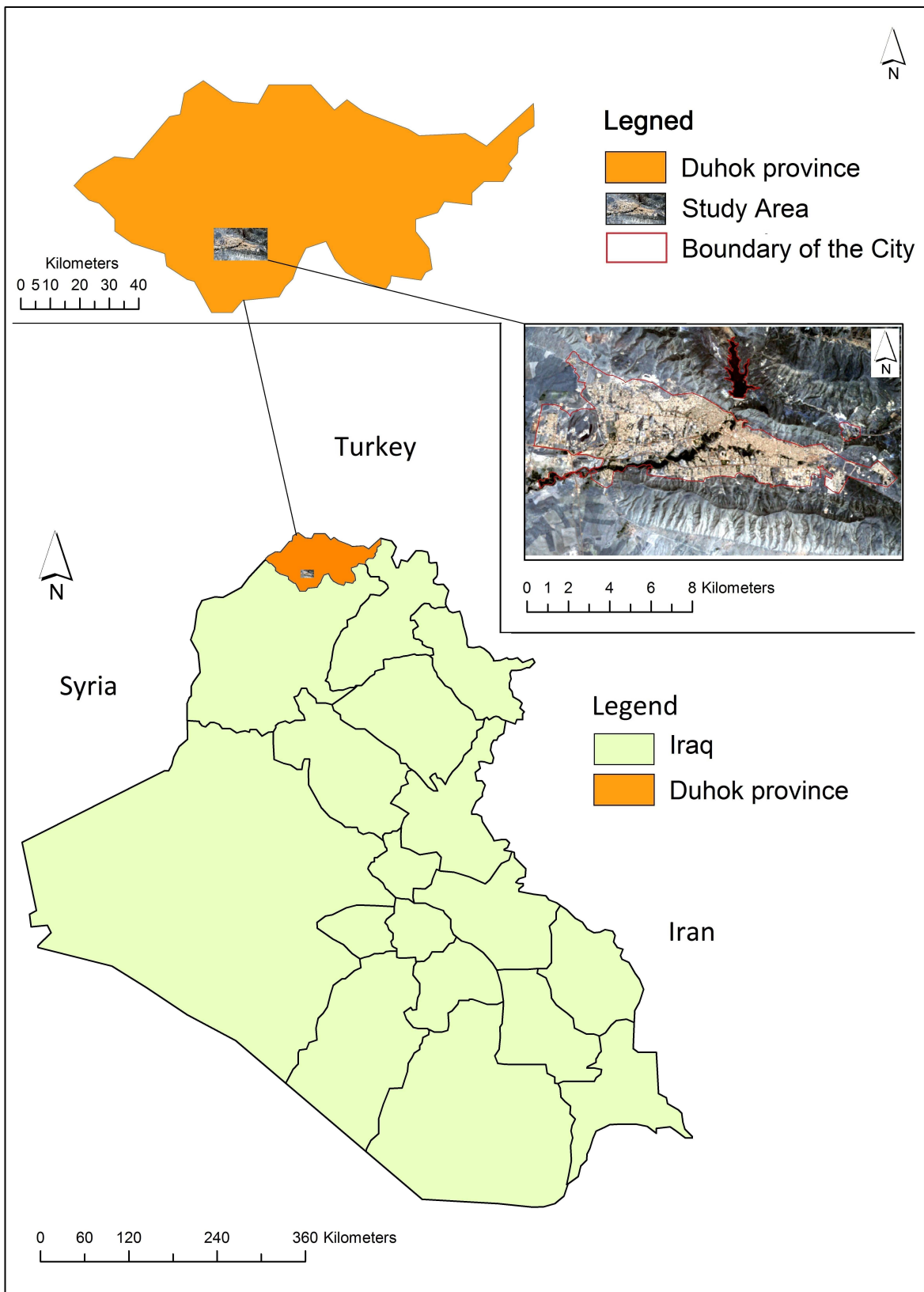
Figure 3.1 Study area.

3.1.1.Geomorphological units

In general, Duhok city falls in the low mountain area and it's roughly (413-1003m) above sea level. Regarding the degree of sloppiness of the city is between (0-43.4 degrees) .As it is shown in the Figure (3.2) and topographical features of Duhok could be divided into three main units:

3.1.1.1. Mountains

Duhok is located between two mountains. The one to the north and east-north is called (Bekher) and the one to the south-west is (Zawita) mountain. The city and due to these mountains has taken a linear shape and very few areas of these two mountains fall into the research area.

3.1.1.2. Hilly areas

This topographical region is clearly seen in the north and western areas of Duhok city. Specifically Zanko region in the west and also the regions (Qasara, Shandokha, Azadi, Se Grka, Bin Tika ,Ronahi, and Peshangaha) in the southern area. This unit is different from others because of the degree of slope (5-15 degrees).

3.1.1.3.Plains: (Flat Areas)

Plain areas are known for the low degree of slope which is usually less than (5 degrees). And it's located in the central and western areas of the research location, especially in the region of (Bahdinan, Masika Roshava, Maltai Sarw, Maltai Zhwrw and Tanahi)
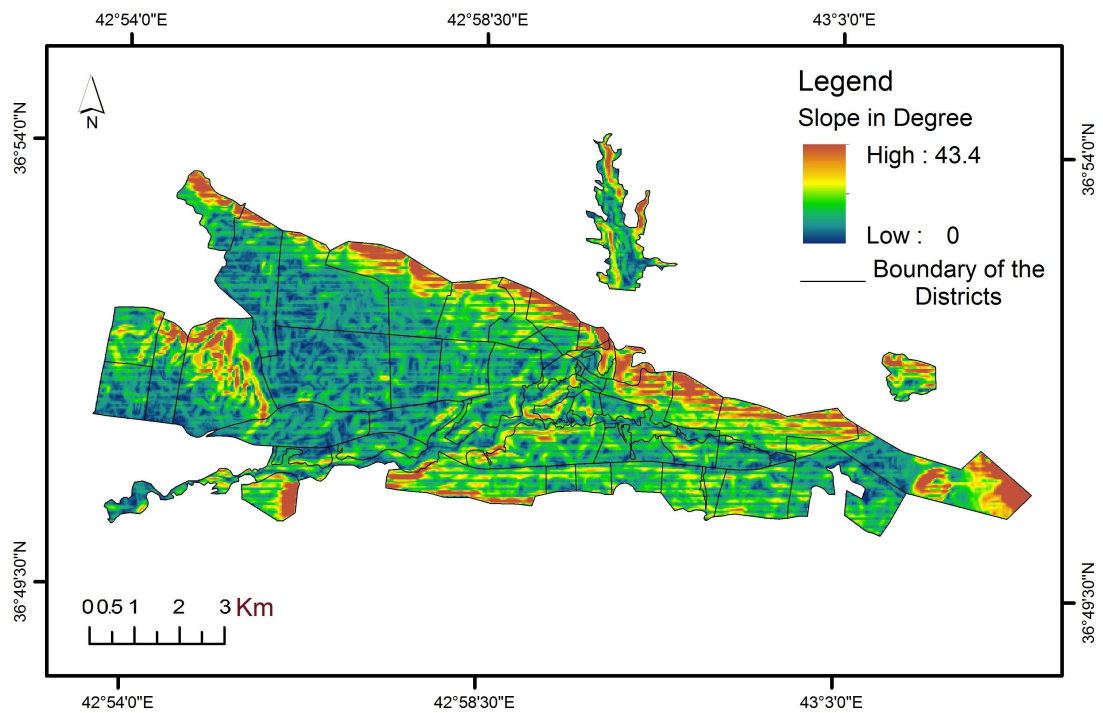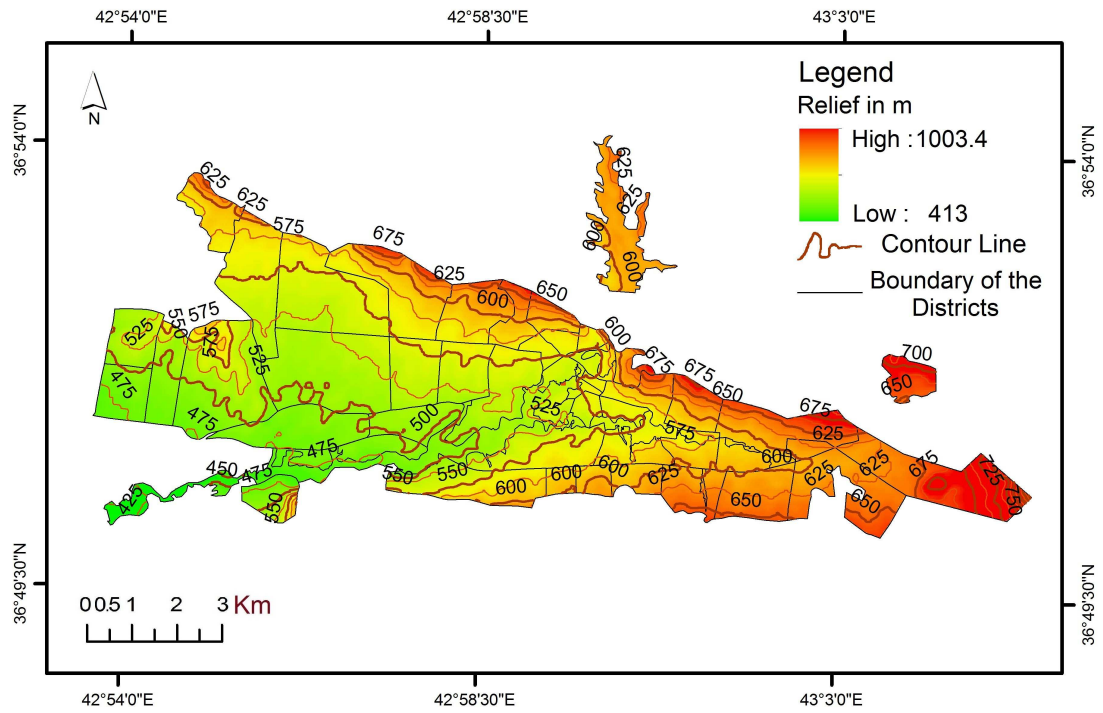
Figure 3.2 Topographic map of the study area

3.2. Data and Materials Used in the Study

The primary data utilized in the current study are two Landsat images obtained from the USGS Earth Explorer website, and Geo-referenced to UTM zone 38, WGS 84. Both images are from Landsat-5 TM; the first image downloaded was taken in June 1998 and the second in June 2011. A gap of 13 years between the images was chosen as being sufficient to find out urban expansion and its affection LST. In addition, secondary data and materials used in this study are clarified by detail in Tables 3.1 and 3.2.

Table 3.1 Landsat-5 TM metadata

Satellite	Landsat TM 5	Landsat TM 5
Date	1998-06-13	2011-06-17
Time	10:22:39 AM	10:34:05 AM
Image ID	LT51700341998164XXX01	LT51700342011168MOR00
WRS Path	170	170
Row	34	34
Projection	UTM Zone 38	UTM Zone 38
Ellipsoid	WGS 84	WGS 84

Table 3.2 GIS files and secondary data used in this study

	Description
Duhok map	This is an ArcGIS shape file which contains information about the names of the main districts and the shape of the city boundary.
Map of latest master plan of the city	This is in PDF file format. It describes and shows the main land uses in the city from now until 2032.
Map of major cities in Iraq	This is an ArcGIS shape file. It contains information on the Iraq boundary, the main cities and governorates.
Duhok weather station data	This is an Excel file containing climatic parameters recorded from 1998 until 2011. These parameters are: humidity, temperature, rainfall.

3.3. Software Used

ERDAS IMAGINE 2010 version 9.2 and ArcGIS 10.0 were used to analyse the images, and to evaluate the results and mapping. Microsoft Excel was used for statistical and regression analysis purposes, and for producing charts and graphs.

3.4. Analysing Satellite Images

Two methods were used to perform the analysis of the satellite images. In general, the first method consisted of two different processes. These processes are as follows: firstly, the images were classified by using supervised classification, and NDVI values with LST were extracted for both images. Secondly, the raster files were converted and inputted into the GIS environment to facilitate easy calculation and the manipulation of the numerical results by working on attribute tables using the ArcGIS software. Figure (3.3) shows the general workflow involved in analysing the satellite images.
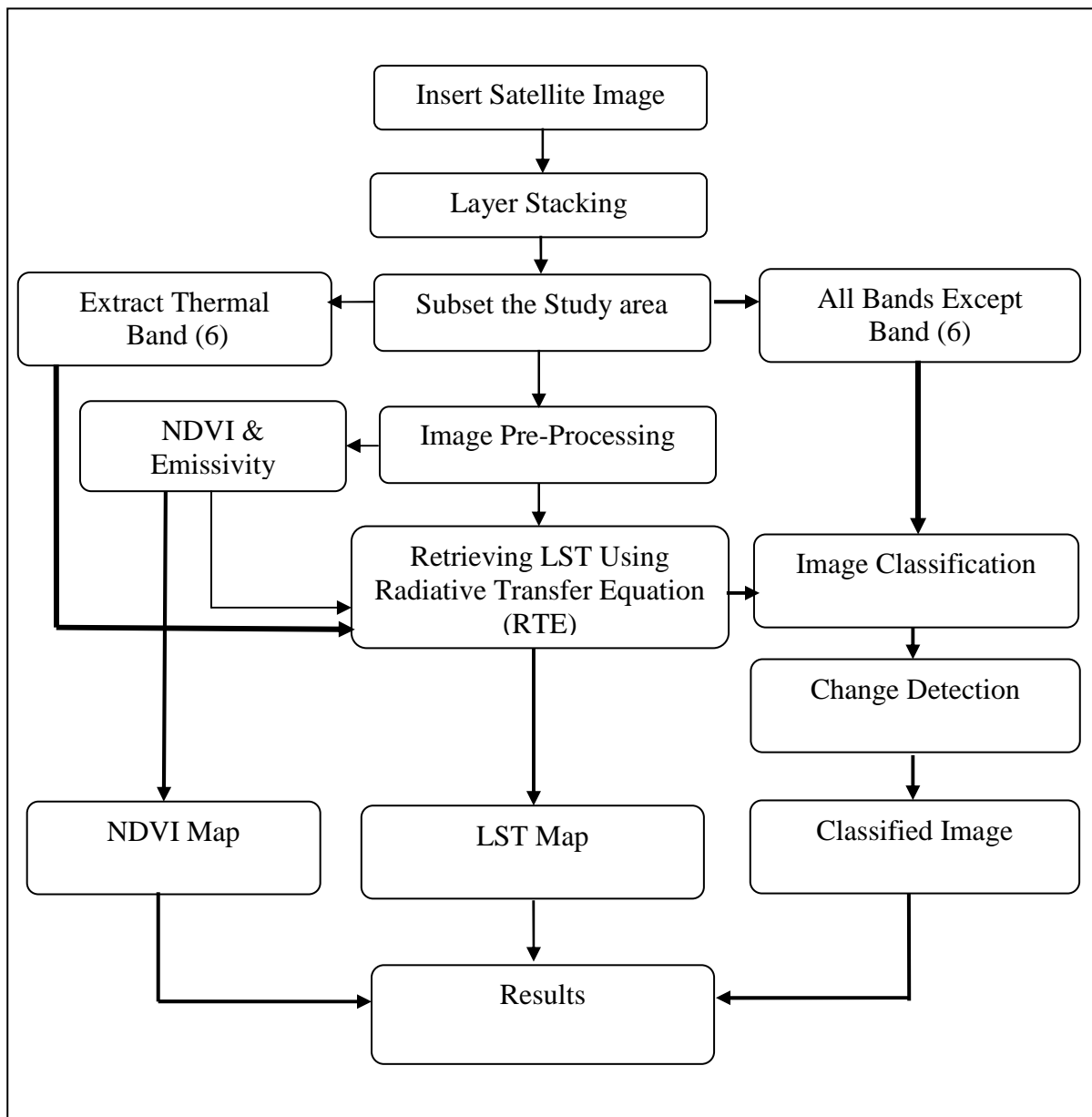
Figure 3.3 General workflow of analysing satellite images.

3.4.1. Layer stacking

Landsat-5 TM has 7 different bands, each of which is stored separately in a Geo TIFF file format. Thus, combining all these bands in a single image, permits analysis using band combinations and enhances visual interpretation. Figure (3.4) shows the images after layer stacking of all Landsat-5 TM bands (1 to 7 with the exception of band 6) has been performed.
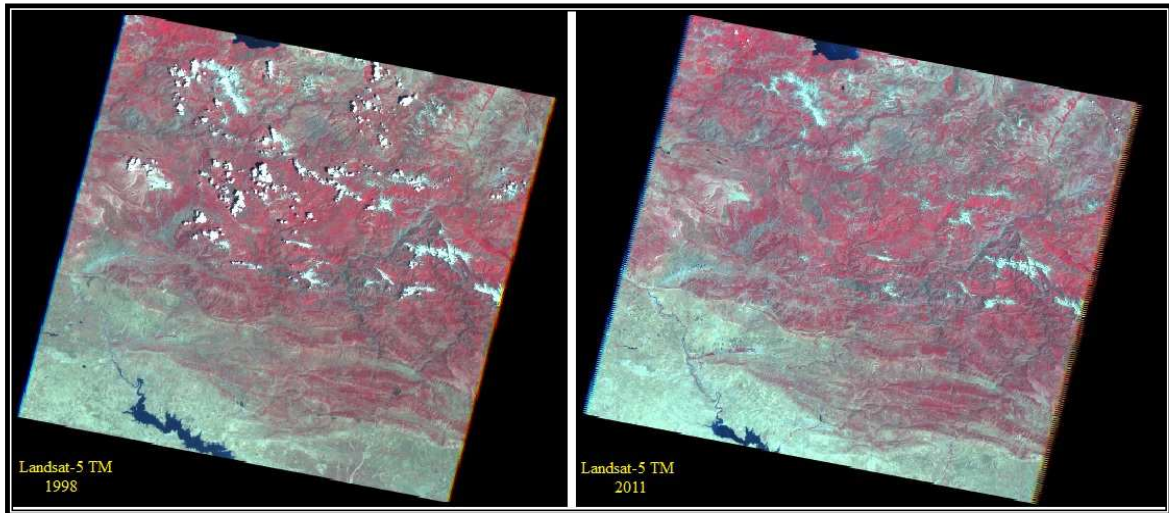
Figure 3.4 Results of layer stacking process for the Landsat images

3.4.2. Subset of the study area

Due to the large size of the original Landsat images, a subset tool in ERDAS IMAGINE was used to select only the area of interest, which in this case is Duhok city. Preparing the subset area is not a difficult task in the context of remote sensing. However, it is extensively recommended in the literature that a properly selected subset should be large enough to provide the context required for the specific analysis (Campbell and Wynne, 2011).Therefore, the subset area selected is encompassed by longitudes 42° 53' 12", 43° 05' 39" and latitudes 36° 54' 19", 36° 48' 33", which gives a total area selected of about 20258.10 Hectares .

3.4.3. Image pre-processing

In this study, image enhancement was used as a part of the image pre-processing. Lillesand *et al*. (2008) state: "The goal of image enhancement is to improve the visual interpretability of an image by increasing the apparent distinction between the features in the scene". As a result, tasselled cap (TC) transformation was employed as a method of

image enhancement. TC is based on measuring the brightness and albedo, which is extracted from the responses of all Landsat-5 TM bands except for the thermal band (Armenakis *et al*., 2003). According to Gao (2009) and Tso and Mather (2009), there are two main advantages for the analyst in employing a TC transformation. Firstly, it makes the classification process less complex by reducing the dimensionality of the feature space. Secondly, it is able to represent specific concepts of the axes of the feature space (brightness, greenness and wetness) because TC transformation is based on the rotation of the axes, and therefore differences among the pixels become distinguishable in the output image (see Figure (3.5)). Thus, the use of TC transformation with Landsat data is strongly advocated in the literature because of its ability to account for more than 90% of the spectral variability present in any given scene, as demonstrated in work by Armenakis *et al*. (2003), Healey *et al*. (2005), Huang *et al*. (2010) and Kiage *et al*. (2007). TC transmutation is known as a useful tool for pressing and squeezing spectral info into a few groups associated with the characteristics of a physical scene (Crist and Cicone, 1984). A TC transformation indicator was computed from the information of the six linked TM bands. Three out of the six TC transformation bands often used are:

Band 1 (Brightness: measure of variations in soil reflectance)

Band 2 (Greenness: measure of variations of vegetation vigour and abundance)

Band 3 (Wetness: interpolation of soil and canopy moisture)

Table 3.3 Coefficients for the Tasselled Cap functions 'brightness', 'greenness 'and 'wetness' for Landsat-5 Thematic Mapper bands 1–5 and 7.

TM bands	B1	B2	B3	B4	B5	B7
Brightness	0.3037	0.2793	0.4343	0.5585	0.5082	0.1863
Greenness	-0.2848	-0.2435	-0.5436	0.7243	0.0840	-0.1800
Wetness	0.1505	0.1793	0.3299	0.3406	-0.7112	-0.4572

Source: Mather (2004, p.147)
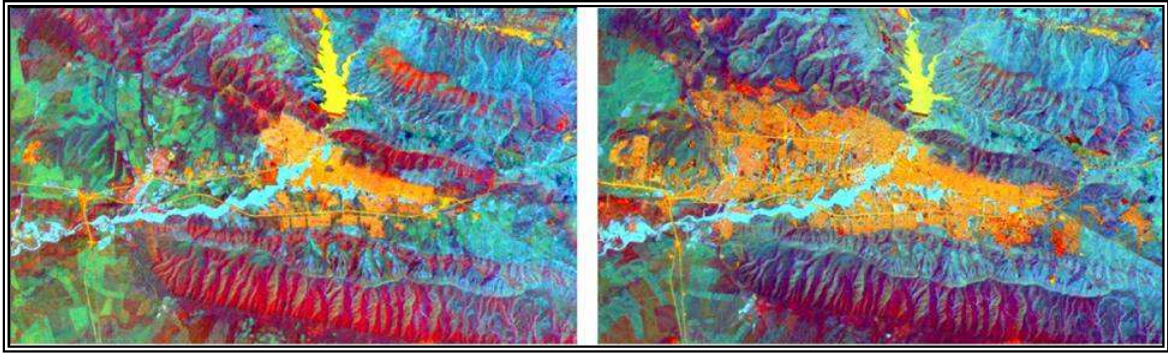
Figure3.5 Results of TC transformation: Urban is represented in yellow, dense vegetation is represented in sky blue, sparse vegetation is represented in turquoise and cadet blue, agriculture is represented in sea green and dark olive green, water is represented in yellow, and other land use is shown as purple or dark red. Left image is 1998; right image is 2011.

3.4.4. Image classification

The main aim of this classification image has to assign the digital pixel values of satellite images into different land cover classes (Mather, 2004). Moreover, image classification can be an automatic process involving assigning pixels to specific groups of known classes based on analyst information and external data sources to identify each land class (ERDAS FILE GUIDE, 2001). In this case, to attain the study objectives, monitored categorization has been employed to categorize land cover classes. So, there are six types of land cover and they are: urban, dense vegetation, sparse vegetation, agriculture, water and other. Figure (3.6) illustrates the steps of supervised classification used in this study:
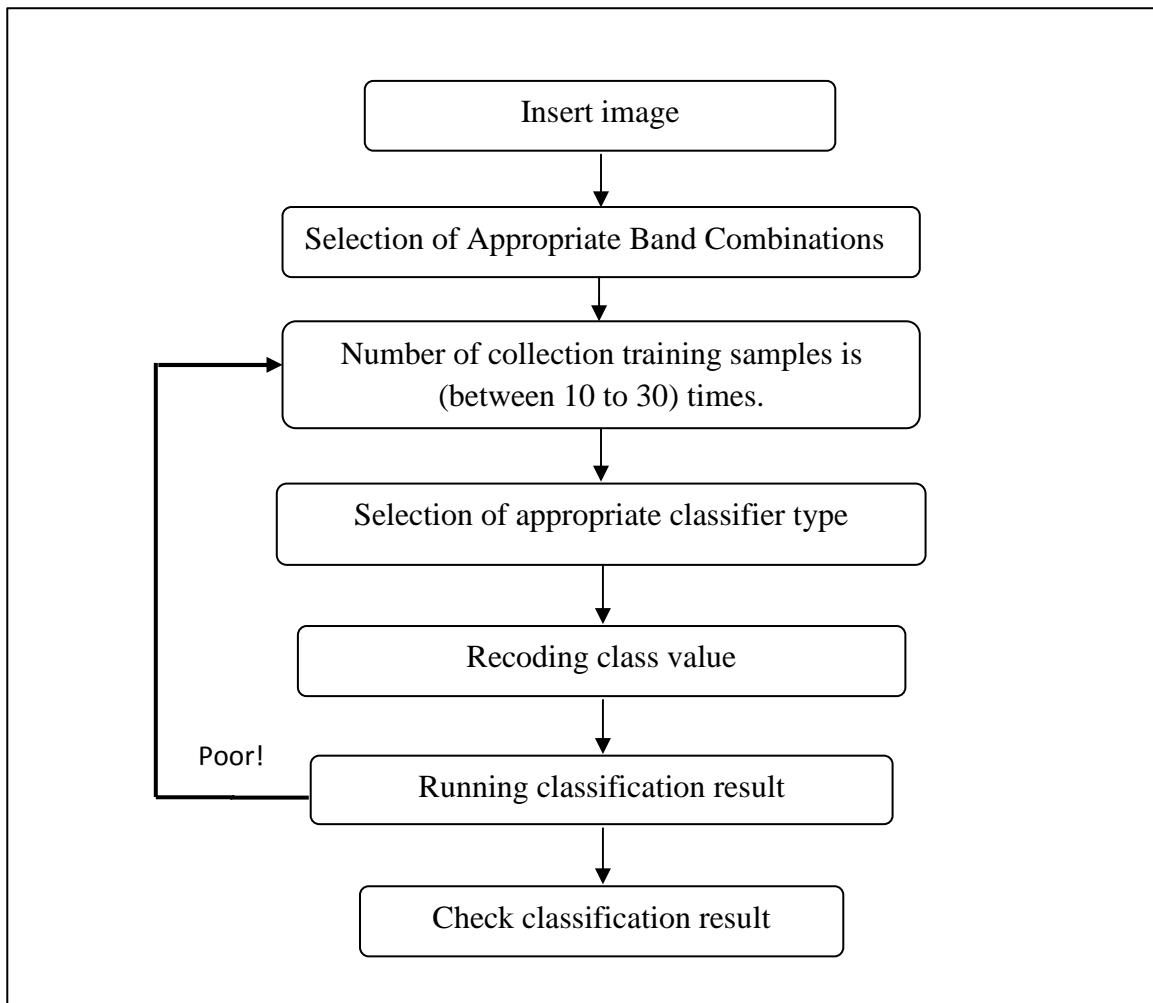
Figure 3.6 General workflow of supervised classification stages used in this study.

3.4.4.1. Selection of appropriate band combinations

The standard false colour composite was used in this study. This consists of bands 3 (red), 4 (near-infrared) and 2 (green). These band combinations are the most appropriate for use in the process of supervised classification using Landsat-5 TM images (Lillesand *et al.*, 2008; Saleh, 2011). Shades of blue, dark slate grey or cyan blue refer to man-made areas or urban areas, shades of red represent dense vegetation land cover, sparse vegetation is light green, different shades of dark green refer to agriculture, dark blue refers to water, and other land forms are represented between different shades of dark to light brown and alice blue (Figure 3.7).

Figure 3.7 Band combination (4, 3, and 2).Left for 1998 and right for 2011.

3.4.4.2. Collecting training data

Supervised classification is informally described as the procedure of using samples of recognized identity. It works based on spectral pattern recognition of each land cover type represented by each pixel in the satellite image (Chuvieco and Huete, 2010; Campbell and Wynne, 2011). In other words, the performance with regard to supervised classification is strongly relying upon how good the analyst is capable to model the target class dissemination (Tso and Mather, 2009). For this reason, the collection of an appropriate training sample is extremely significant step in the process of supervised classification, and assembling accurate training data is the path to the success of the whole process. Assembling the training data requires effort in terms of combination between of art and science. Therefore, four different points were taken during the selection process with regard to the training sample, based on Gao's (2009) recommendations:

i. As mentioned earlier, the main concept of supervised classification is to assign pixels into different land cover classes. As a result, the quantity of pixels chosen for each class during the training stage plays an important role in obtaining correct results. For example, the more extensively a land cover type is distributed over the scene, the more pixels should be selected for this class. Lillesand *et al.* (2008) suggested using more than 20 training samples for each land cover class, with 40 pixels within each training sample. In addition, Mather (2004) stated that if a particular classifier type likely to be the most common, the quantity or number of the pixels within the training sample should at least 10 to 30 times the number of features for each class. Therefore, this study attempted to follow these criteria as much as possible in terms of collecting training samples.

ii. It is common for the training sample to be selected by delimiting the boundary around the target pixels. As a result, the size of these samples also has a great impact on the final result. In fact, there is no standard rule for determining the physical size of these training samples. However, the variation of the classes may identify the size of each sample. For example, if the study area has only one body of water, the sample size may cover the whole of the body of water instead of using smaller samples within the same location.

iii. The location of training samples is another important point. The analyst should collect samples from the whole scene in order to avoid missing particular classes or pixels relating to a specific land cover class (Chuvieco and Huete, 2010).

iv. The degree of uniformity in terms of spectral radiance has the greatest impact on the classification results, i.e., pixels chosen for a class should ideally all exhibit a unimodal distribution in their values in terms of the spectral band used (Gao, 2009).

However, supervised classification requires some additional inputs before the application of any algorithms. These inputs might be gathered from a field where you work on through, air photo analysis, reports, or from the study of appropriate maps of the area of interest (Mather, 2004).Therefore, the image analyst should have fundamental reference data and a comprehensive understanding of the geographical area (Lillesand *et al*., 2008). Ancillary data are strongly recommended during the classification process with regard to urban areas, in order to enhance the contextual interpretation of the spectral and spatial satellite data (Chuvieco and Huete, 2010; Mesev, 2010).Therefore, ancillary data from Google Earth and maps of the Duhok city master plan were used during the process of collecting training data, together with the researche's knowledge of the city.

The data from Landsat-5 TM have medium spectral resolution, and because of homogeneous pixels and the complex structures of urban spectral characteristics, it is difficult to distinguish easily between all types of land cover within an urban area. Thus, an accurate classification of different land cover types representing urban areas is a difficult task with regard to using Landsat imagery data (Bhatta, 2010; Mesev, 2010). For this reason, in order to achieve the study objectives, only the required classes were identified.

The images for both 1998 and 2011 were divided into six classes with regard to the main objectives of this study. These are: urban, dense vegetation, sparse vegetation, agriculture, water and other. Urban land includes all of the man-made types, such as residential, industrial, institutional, transportation and buildings. Dense vegetation and

sparse vegetation are characterized as those vegetation areas where the land is dominated by grasses rather than large shrubs or trees, while sparse vegetation can vary in height from very short to quite tall. However, based on NDVI values, we divided the vegetation classes into two classes - dense and sparse - based on the values of NDVI with less than 0.100 representing sparse vegetation, and values up to 0.100 representing dense vegetation. In this stud agricultural land defined as the share of the land area that is arable (farming), therefore, the land actually under annually-replanted crops in any given year. In other words, the land is replanted annually. In addition, a water body in this study identified as any significant accumulation of water In general, the majority of geographical features are happening naturally, but some have been man-made (John Wiley & Sons in 2007). Other class represents barren land and unclassified areas. Barren land is defined by Anderson *et al*. (1976) as: "…land of limited ability to support life and in which less than one-third of the area has vegetation or other cover. In general, it is an area of thin soil, sand, or rocks".

Due to the study objective of attempting to find a link between land cover classes and LST, especially the selected classes in our study and LST, training data were collected based on the criteria noted above, together with external data sources and the analyst's experience of the study area. The reason for the division into the above-mentioned classes is to facilitate the study's objective, which is to show the impact of urban expansion on LST, and the relationship between different land covers and LST.

3.4.4.3. Selection of appropriate classifier type

There are three main classifier methods: parallel-piped, minimum distance and maximum likelihood classifiers. As Gao (2009) says; "…all of these classifiers have advantages and limitations, but the last two are the most widely used with Landsat data". In this research, the classifier maximum likelihood has been used. Tso, has defined The techniques of the maximum likelihood classifier as: "The probability of a pixel belonging to each of a predefined set of classes is calculated and the pixel is then assigned to the class for which the probability is the highest" (Tso and Mather, 2009).

3.4.4.4. Recoding class values

The purpose of using recoding in our study is to allocate another class number for the all classes or one class of a presenting img. file format. According to our classification of classes, the recode process resulted in creating an output file using the new class numbers. In general, the aim of using the recoding process could be summarize in the three

following aspects: in order to decrease the classes, to integrate the classes, and to determine a new class values for the presenting classes utilizing ratio, ordinal or interval class numbering system is allow the recoding to be conduct for determine classes for the suitable values. Recoding is usually carry out for simplifying the following steps. In order to make later steps easier. In this study it is used to facilitate the procedure of finding out the LST for each class.

3.4.4.5. Estimation of classification accuracy

The aim of collecting training data sets is to oversee the classification process as required by the analyst. However, it is significant here to guarantee that the training data are sufficient, and that there are no unrepresentative pixels included in the training data sets (Tso and Mather, 2009).Therefore, the process of classification is not complete until its accuracy has been assessed. In the other words, accuracy assessment establishes how good the analyst's classification of the image is (Lillesand *et al*., 2008). Thus; "…accuracy is a working sense, as the degree (often as a percentage) of correspondence between observation and reality" (Levin, 1999). In general, accessing the accuracy of remote sensing images can be done by two methods, in the form of positional and thematic assessment (Congalton and Green, 2009). With positional accuracy assessment, the analyst only deals with the spatial distribution of the features on the map and on the ground in order to find out to what extent the features are distributed in a real scene. However, with thematic assessment, the analyst deals with the labels or attributes of the features of a map, and measures whether or not the mapped features or classified image labels are likely given the true feature label. In this case, the most common and widely used method is error matrix (confusion matrix). Error matrix works by choosing a group of random points in the classified image, and comparing them with a real scene in the image. Thus, to assess the accuracy, a total of 240 random points was collected for each image separately.

3.4.5. Change detection

Change detection is a key to change thematic data structure information that can lead users to a better concrete insights into the core processes relating to land cover and land use change than the knowledge attained from continuous change (Singh *et al*., 2013). Such an approach compares LC data to available information for each class. In ERDAS imagine software, we can use two tools for change detection (the Change Detection operation from Utilities and the Matrix operation from the GIS Analysis menu). In this

research I used the second tool (the matrix) to analyze change detection. The change detection technique involving supervised image classification with the highest overall accuracy was used to figure out and explain the changes in LC among two terms: 1998 and 2011. Changes in the quantitative aerial data of the overall land use/cover in each category were compiled. The quantification of change for the categories analyzed is shown in Table (4.3). This reports the relative statistics, aggregated for each class. The final change map is created by clustering and labeling the changed matrix classes.

3.5. Calculating and Retrieving Land Surface Temperatures

As mentioned in the literature section, there are several methods for retrieving land surface temperatures using thermal infrared band from remote sensing instruments. However, the following three methods are the most widely used according to the literature: 1) The single-channel method: this method is suitable for those sensors that have only one thermal band such as Landsat TM/ETM+. 2) The two-channel or split-window method: this method is only suitable for sensors having at least two thermal bands such as ASTER & MODIS. 3) The temperature and Emissivity Separation (TES) method developed by Gillespie *et al*. (1998). Hence, in our study the single-channel method was applied for retrieving land surface temperatures since the Landsat TM/ETM+ sensor carries only one thermal band (B6). At the core of this method is the equation transferring thermal radiance, which usually concentrates on converting satellite digital values to a radiometric value by using the satellite low and high gain values (Markham and Barker, 1986). In addition, it is important to note that the differences in the literature also appear in relation to using single-channel methods. This is because there are three different methods that can be applied with the single channel method. These are: i) the Radiative Transfer Equation (RTE), ii) the Mono-window algorithm of Qin *et al*.'s (2001) algorithm, and iii) Jimenez-Munoz and Sobrino's (2003) algorithm. In this study, RTE, the first method associated with single-channel methods, has been used. The single-channel method, however, requires some atmospheric parameters which are usually derived from MODTRAN radiative transfer. However, these parameters are quite difficult to retrieve. A simple and quick way to overcome this problem is to use the online atmospheric correction parameter calculator developed by Barsi *et al*. (2005). These parameters could be retrieved with the Atmospheric Correction Parameter Calculator and is available online at http://atmcorr .gsfc.nasa.gov/.Figure (3.8) shows the general workflow involved in terms of describing Land Surface Temperatures (LST).
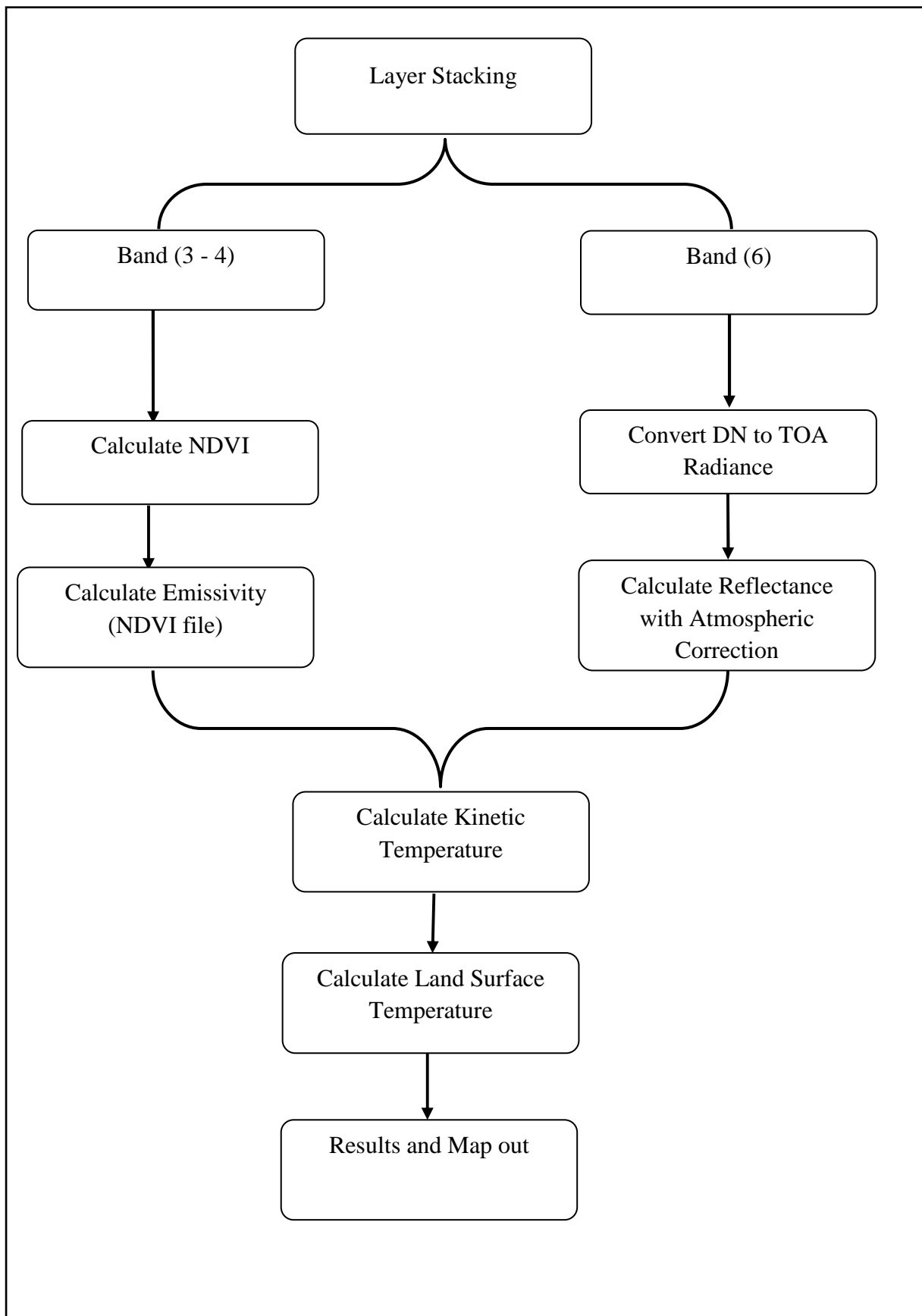
Figure 3.8 General workflow of converting Landsat Thermal band to Land Surface Temperature.

3.5.1. Conversion of digital values to radiance

The first step is converting thermal band values to radiance. In general, any object with a temperature above absolute zero Kelvin emits thermal electromagnetic energy. The signals received by the thermal sensors of Landsat TM/ETM+ are stored and represented as digital numbers (DN). Eq. (1) is used to convert these DNs to space reaching radiance or top-of-atmosphere (TOA) radiance measured by the instrument (Markham and Barker, 1986; Thome *et al*., 1997; Chander *et al*., 2002; Chander and Markham, 2003) (as cited in Oguz,2013):

$$L_\lambda = \frac{L_{max} - L_{min}}{QCAL_{max} - QCAL_{min}} (DN - QCAL_{min}) + L_{min} \tag{1}$$

Where: L_λ = spectral radiance at the sensor's aperture in $W/(m^2 \ sr \ \mu m)$; QCALmax = the highest point of the rescaled radiance in DN; $QCAL_{max}$ = the lowest point of the rescaled radiance in DN (1 for LPGS, 0 for NLAPS); L_{max} = the TOA radiance that is scaled to $QCAL_{max}$ in $W/(m^2 \ sr \ \mu m)$; L_{min} = the TOA radiance that is scaled to $QCAL_{min}$ in $W/(m^2 \ sr \ \mu m)$.

3.5.2. Conversion to reflectance with atmospheric correction

In this step the radiance value obtained in the first equation will be converted to reflectance with atmospheric correction. This method was developed by Chavez (1996) and its main advantage is that the data necessary in order to carry out the atmospheric correction are obtained from the image itself. The atmospherically corrected reflectance of the earth is computed in Eq. (2) (Sobrino *et al*., 2004) (as cited in Oguz,2013):

$$\rho_P = \frac{\pi.(L_\lambda - L_h).d^2}{ESUN_\lambda.\cos\theta_s.\tau} \tag{2}$$

Where: ρ_P = atmospherically corrected unitless planetary reflectance; L_λ = spectral radiance at the sensor's aperture; L_h = radiance resulted from the interaction of the electromagnetic radiance with the atmospheric components (molecules and aerosols); d = earth-sun distance in astronomical units; $ESUN_\lambda$ = mean solar exo-atmospheric irradiances; θ_s = solar zenith angles in degrees; τ = the atmospheric transmissivity.

L_h can be obtained according to Eq. (3):

$$L_h = L_m - L_1\% \tag{3}$$

Where: L_m = the radiance that corresponds to the dark object DN value; $L_1\%$ = 1 percent of the theoretical radiance of a dark object.

Lm cab be computed in Eq (4)

$$L_m = L_{min} + DN_{min} \left(\frac{L_{max} - L_{min}}{QCAL_{max}} \right) \tag{4}$$

Where: DN_{min} = the dark object DN value (minimum DN value).

The term $L_1\%$ is given by Eq. (5):

$$L_1\% = \frac{0.01 . \cos\theta s . \tau . ESUN\lambda}{\pi . d^2} \tag{5}$$

τ can be obtained according to Chavez (1996) in Eq. (6):

$$\tau = \cos\theta_s \tag{6}$$

Sobrino *et al*. (2004) compared Chavez's (1996) method to the simplified method for atmospheric correction (SMAC) and found that both methods resulted in similar results. For this reason, Chavez's (1996) method is used for atmospheric correction.

3.5.3. Calculation of the Normalized Difference Vegetation Index (NDVI)

The Normalized difference vegetation index NDVI is a widely used parameter in studies on LST. Because NDVI is less sensitive to the changes of atmospheric conditions than the other indices, it has become the most widely used for monitoring vegetation status (Tso and Mather, 2009). The purpose of using NDVI in this study is to evaluate the correlation between LST and NDVI, and derive land surface emissivity from the NDVI values; which is a required parameter when using the a split window algorithm. The basis of the NDVI is a rational calculation between two of the most important Landast-5 TM bands. These bands are near-infrared (NIR) band 4 and Red (R) band 3 (Gao, 2009; Liu and Zhang, 2011).. the reason for using these two bands is that healthy vegetation or green leaves have more than 60% reflectance, with band 4 between wavelengths 0.7 to 1.3μm. However, with band 3, the red band, the highest value of reflectance reached is 20% k9 between the wavelengths 0.5 to 0.7μm. The following equation was used to extract exact

values of NDVI based on the Landsat-5 TM data bands .NDVI is derived from the atmospherically corrected reflectivity of Landsat TM/ETM+ bands as shown in Eq. (7):

$$NDVI = \frac{\rho_{band4} - \rho_{band3}}{\rho_{band4} + \rho_{band3}} \qquad (7)$$

Where: ρ_{band4} = the spectral reflectance of near infrared band (band 4); ρ_{band3} = the spectral reflectance of red band (band 3).

3.5.4. EMISSIVITY and NDVI

3.5.4.1. Land Surface Emissivity Estimation using the NDVI thresholds (NDVITHM) method

Radiation emitted by ground objects is measured in order to estimate their temperature by use of thermal infrared wavelengths. Therefore, these measurements provide the radiant temperature of a target body and thus, the radiance is strongly dependent on the emissivity of the target (Prakash, 2000). For this reason, it is quite important to retrieve emissivity values in order to get accurate results in terms of retrieving LST. "Emissivity (ε) is a proportionality factor that measures black body radiance (Planck's law) to predict emitted radiance and its efficiency in transmitting thermal energy across the surface into the atmosphere. In this sense, (ε) must be known in order to estimate land-surface temperature accurately from radiance measurements" (Sobrino *et al*., 2008) i.e., emissivity is an essential parameter in the study of LST. Calculating land surfaces on Earth does not measure black bodies perfectly. Thus, thermal emissivity of the land surface must be estimated for the area being studied (Gartland, 2008). However, an accurate estimation of ground emissivity remains a difficult task. Several methods of retreiving acceptable results of ground emissivity have been proposed by various researchers (Qin *et al*., 2001). The work by Zhang *et al*. (2006) proposed a very good estimation for the emissivity of different land surfaces using three different methods. These methods are NDVI values, image classification and ratio values of vegetation and bare ground. However, using NDVI is the proper method as Ifatimehin (2007) says: "…land emissivity is more relative with the densely vegetated surface and high heterogeneous surface". In addition, the methods-based image classification developed by Zhang might be

28

impossible to use with Landsat data because this method needs high-resolution data. Thus, in this study, emissivity values were extracted by using NDVI values.

The land surface emissivity (ε) is derived by the NDVI Thresholds Method. This method obtains the emissivity values from the NDVI considering different cases as follows (Sobrino et al., 2004):

$\varepsilon = \varepsilon_{soil}$ if NDVI<0.2

$\varepsilon = \varepsilon_{veg}$ if NDVI>0.5

$\varepsilon = (\varepsilon_{veg}. P_V) + \varepsilon_{soil} (1-P_v)$ if 0.2≤NDVI≤0.5

where: ε_{soil} = the soil emissivity; ε_{veg} = the vegetation emissivity; P_v = the vegetation cover fraction.

According to Sobrino et al. (2004), εsoil and εveg were estimated at 0.97 and 0.99 respectively. After using these values in the formulas above, the equation below is formulated:

$\varepsilon = 0.97$ if NDVI<0.2

$\varepsilon = 0.99$ if NDVI>0.5

$\varepsilon = 0.004. P_V + 0.984$ if 0.2≤NDVI≤0.5

P_v is calculated as shown in Eq. (8) (Carlson and Ripley, 1997):

$$P_v = \left(\frac{NDVI - NDVI_{min}}{NDVI_{max} - NDVI_{min}} \right)^2 \qquad (8)$$

where $NDVI_{max} = 0.5$; $NDVI_{min} = 0.2$

Based on these estimations, formula conditional functions in ERDAS IMAGINE software were used to estimate emissivity values for the study area.

3.5.4.2. Land Surface Emissivity estimation using a classification image

Before using this method, the user is required to classify the satellite image (Landsat TM/ETM+) into classes of land use and land cover using one of the image processing packages such as Erdas Imagine, ENVI etc. The LST tool supports a maximum of 10 land use and land cover classes. Each class must be assigned an integer value from 1 to 10 (only if there are 10 classes in the image). After preparing the classified image,

emissivity values for all land use and land cover can be retrieved from the paper written by Snyder *et al*. (1998) and are assigned for each land use and land cover class using the LST tool's "Emissivity Calculation using a Classification File" dialog. Therefore, the classified image and the emissivity values are critical in this method. The final LST result depends solely on the classification accuracy of the classified image and the emissivity values for the land cover classes. A Landsat TM/ETM+ image has a spatial resolution of 30x30 m, which is probably composed of several land objects. For this reason, the emissivity from a pixel is determined by land objects and their emitting directions (Dozier and Warren, 1982) (as cited in Oguz,2013). Many studies have been published estimating the emissivity values of ground objects to mitigate the effect of emissivity on derived LST (Gillespie *et al*., 1998; Snyder *et al*., 1998; Watson, 1992). Snyder *et al*. (1998) states that correction of the effect of emissivity can be achieved by assigning an emissivity value to each land cover category of the classification image. According to the literature, land surface emissivity ranges from 0.950 to 0.990 (Lillesand *et al*., 1994; Nichol, 1994; Snyder *et al*., 1998) (as cited in Oguz,2013).

3.5.5. Calculate kinetic temperature

In this stage the process of removing atmospheric effects will apply, which is crucial for absolute temperature studies. It is well known that the energy emitted from the ground is usually attenuated by the atmosphere (Barsi *et al*., 2005). The effects of the atmosphere in the thermal region are removed by converting space-reaching or TOA radiance to surface-leaving radiance. In this study, an atmospheric correction tool which uses the MODTRAN radiative transfer code developed by Barsi *et al*. (2005) for the thermal band of Landsat TM/ETM+ was applied. This tool estimates three parameters – atmospheric transmission, upwelling radiance, and down-welling radiance. Once these parameters are retrieved, it is possible to convert the space-reaching radiance or TOA radiance to surface-leaving radiance with the Eq. (9) (Barsi *et al*., 2005) (as cited in Oguz,2013) :

$$L_T = \frac{L_\lambda - L_\mu - \tau(1 - \varepsilon)L_d}{\tau . \varepsilon} \tag{9}$$

Where: L_T = radiance of a blackbody target of kinetic temperature T; L_λ = the space-reaching or top of atmospheric radiance; L_μ = the upwelling or atmospheric path

radiance; L_d = the down-welling or sky radiance; τ = the atmospheric transmission; ε = the emissivity of the surface.

3.5.6. Land Surface Temperature calculation

The conversion of DVs to spectral radiance is the next step in converting spectral radiance to satellite brightness temperature (blackbody temperatures) by expressing Planck's function. However, in this study another equation was used, which is similar to Planck's function. This equation was proposed by Markham and Barker (1986): it states that the radiances are in units of W/(m^2 sr μm), while the transmission and emissivity are unitless. The land surface temperature was calculated using the Eq. (10)

$$T = \left(\frac{K_2}{\ln\left(\frac{K_1}{L_T} + 1\right)} \right) - 273.15 \tag{10}$$

Where: T is the satellite brightness temperature in Celsius, K_1 and K_2 are calibration constants of Landsat-5 TM representing at sensor spectral radiances of Landsat TM Band 6, which are 607.76 and 1260.56, respectively; L_T is the satellite spectral radiance retrieved from the first equation - the advantage of using this algorithm lies in being able to use additional parameters to obtain an accurate LST.

3.6. Input and Converting Results into the GIS Environment

Recorded data in remotely sensed images takes the form of pixel values, where each pixel records X, Y information for a ground location. Therefore, this allows the remotely derived information to be used with other data in spatial distributed modeling efforts, such as with GIS (Lindgren, 1985; Jensen and Hodgson, 2004). In other words, the development and unison of remote sensing and Geographical Information Systems (GIS) has led to the multi spatial analysis of data (Chapman and Thornes, 2003).The result of inputting and converting remotely sensed data into the GIS environment allows a variety of numerical and geographical analysis techniques to be employed, such as extracting mean values of LST for each land cover class and districts and mapping out the results in an appropriate manner.

For this reason, in order to achieve the study objectives, GIS techniques were used to analyze and evaluate spatial information. Firstly, all the obtained results were imported into ArcGIS software to facilitate the process of reclassifying the raster images by conversion to a raster-grid. The reason for reclassifying images was to moderate the values in an input to save the changes to a new output raster which produces unique values and clears the background from the class. There are many reasons why we may want to do this, including replacing values based on new information, grouping entries, and reclassifying values to a common scale. Secondly, the LST images are combined with reclassified images for each class through Extract using the mask tool in ArcGis. These steps have been used for each class separately, which counts as a point of strength in terms of this study. Finally, the city districts maps were converted to a polygon in order to extract separate LST values for each district. For this reason, the spatial analysis tool (extract by using the mask tool) was used in ArcGis software. A complete workflow of this step is illustrated in Figure (3.9).

```
                        ┌──────────────────────┐
                        │  Classified Images   │
                        └──────────────────────┘
         ┌──────┬──────────┬──────────┬──────────┬──────────┬──────────┐
         ▼      ▼          ▼          ▼          ▼          ▼
    ┌────────┐┌──────────┐┌─────────┐┌───────────┐┌───────┐┌───────┐
    │ Urban  ││Sparse veg.││Dense veg.││Agriculture││ Water ││ Other │
    └────────┘└──────────┘└─────────┘└───────────┘└───────┘└───────┘
```

```
┌──────────┐┌──────────┐┌──────────┐┌──────────┐┌──────────┐┌──────────┐
│Conversion││Conversion││Conversion││Conversion││Conversion││Conversion│
│to Raster-││to Raster-││to Raster-││to Raster-││to Raster-││to Raster-│
│  Grid    ││  Grid    ││  Grid    ││  Grid    ││  Grid    ││  Grid    │
└──────────┘└──────────┘└──────────┘└──────────┘└──────────┘└──────────┘
```

```
┌──────────┐┌──────────┐┌──────────┐┌──────────┐┌──────────┐┌──────────┐
│Reclassify││Reclassify││Reclassify││Reclassify││Reclassify││Reclassify│
│Grid Data ││Grid Data ││Grid Data ││Grid Data ││Grid Data ││Grid Data │
└──────────┘└──────────┘└──────────┘└──────────┘└──────────┘└──────────┘
```

```
┌──────────┐                    ┌────────────┐
│  City    │                    │   LST      │
│Districts │                    │  IMAGE     │
│  Maps    │                    │            │
└──────────┘                    └────────────┘
     │
     ▼
┌──────────┐        ┌──────────────────────┐
│Convert To│        │   Extract by Mask    │◄───────
│ Polygon  │        └──────────────────────┘
└──────────┘
     │
     ▼
┌──────────┐
│Extract by│◄──────────────────────────────────
│  Mask    │
└──────────┘
```

```
┌──────────┐┌──────────┐┌──────────┐┌──────────┐┌──────────┐┌──────────┐
│Urban-LST ││  Dense   ││ Sparse   ││Agriculture││Water-LST ││Other-LST │
│ Output   ││ Veg.-LST ││ Veg.-LST ││  -LST    ││ Output   ││ Output   │
│          ││ Output   ││ Output   ││ Output   ││          ││          │
└──────────┘└──────────┘└──────────┘└──────────┘└──────────┘└──────────┘
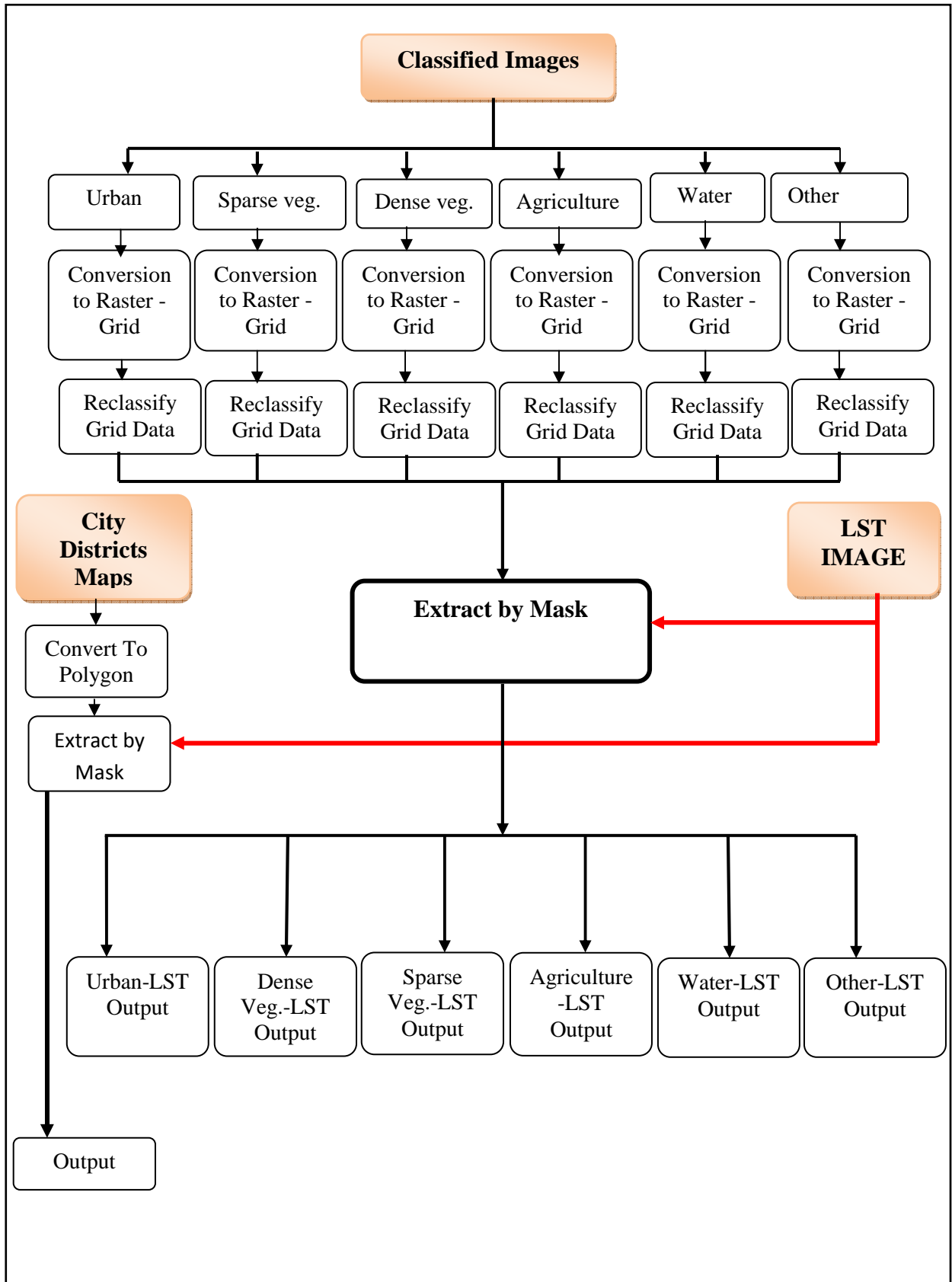```

```
┌──────────┐
│  Output  │
└──────────┘
```

Figure 3.9 General workflow of converting obtained results from raster file format into

vector file format in GIS environment .

4. RESULTS AND DISCUSSIONS

4.1. Classification Results

In order to classify land cover classes and detect any change among the different land cover classes between 1998 and 2011, a supervised classification was utilized based on Landsat-5 TM. The results of the classification indicate that all of the classes vary between 1998 and 2011. As it is shown in the Figure (4.1) which represents the main land cover types. The colour red represents urban land including buildings and roads, dark green represents all types of dense vegetation, light green represents sparse vegetation, gold represents agriculture land, blue represent accumulation of water. Brown represents other land which is non-built up or barren land with insignificant vegetation land as well as thin soil, sand, or rocks.

It is noted that in 1998 the largest area was covered by sparse vegetation which made up around 32.27% of the total area. However, in 2011 sparse vegetation land cover had declined by to just over 29.03%. On the other hand, significant changes were noted during this period of time in urban land, which increased from 5.98 % in 1998 to 17.62 % in 2011. The increasing trend in urban land is due to the economic and political changes which occurred in this region after a semi-autonomous government structure was introduced. It appears that the city experienced a fast and large-scale expansion of urban land compared with other land cover types. In contrast, dense vegetation decreased during the years under investigation, as we can see, from 31.69% to 19.59% as a result of: i) the impact of climate change such as drought which has faced the entire region since the 1990s ii) as we can see from the classified images, there is dense vegetation located around the river going through the city but in 2011 the river dried up so there was no water. Therefore, vegetation around the river decreased between these years. Likewise, agriculture land cover decreased from 14.27 % to 12.31% as a result of vast expansion of the built up land area upon other land cover types. The remaining two types of classes increased from 1998 to 2011, these are water and other classes. The water land cover increased from 0.66 % to 0.69 % because the bodies of water represented in this study focus on the water collected by a man-made dam which collects water during the rainy season, and because the two images used in this study were acquired almost in the same month. Hence there is no evident change in the bodies of water. The remaining land cover increased from 15.13 % to 20.76 %. (see Table (4.1) and Figure (4.2).

Table 4.1 Summary results of LU/LC change between 1998 and 2011.

Class name	Area In (ha) 1998	Area in (ha) 2011	Coverage % 1998	Coverage % 2011	Changes %	Remark
Urban	1212.93	3569.58	5.98	17.62	11.64	Increase
Dense Vegetation	6411.87	3969.63	31.69	19.59	12.1	Decrease
Sparse Vegetation	6537.33	5880.15	32.27	29.03	3.24	Decrease
Agriculture	2892.6	2493.63	14.27	12.31	1.96	Decrease
Water	135.54	139.32	0.66	0.69	0.03	Increase
Other	3067.83	4205.79	15.13	20.76	5.63	Increase
Sum	20258.10	20258.10	100	100	34.6	-
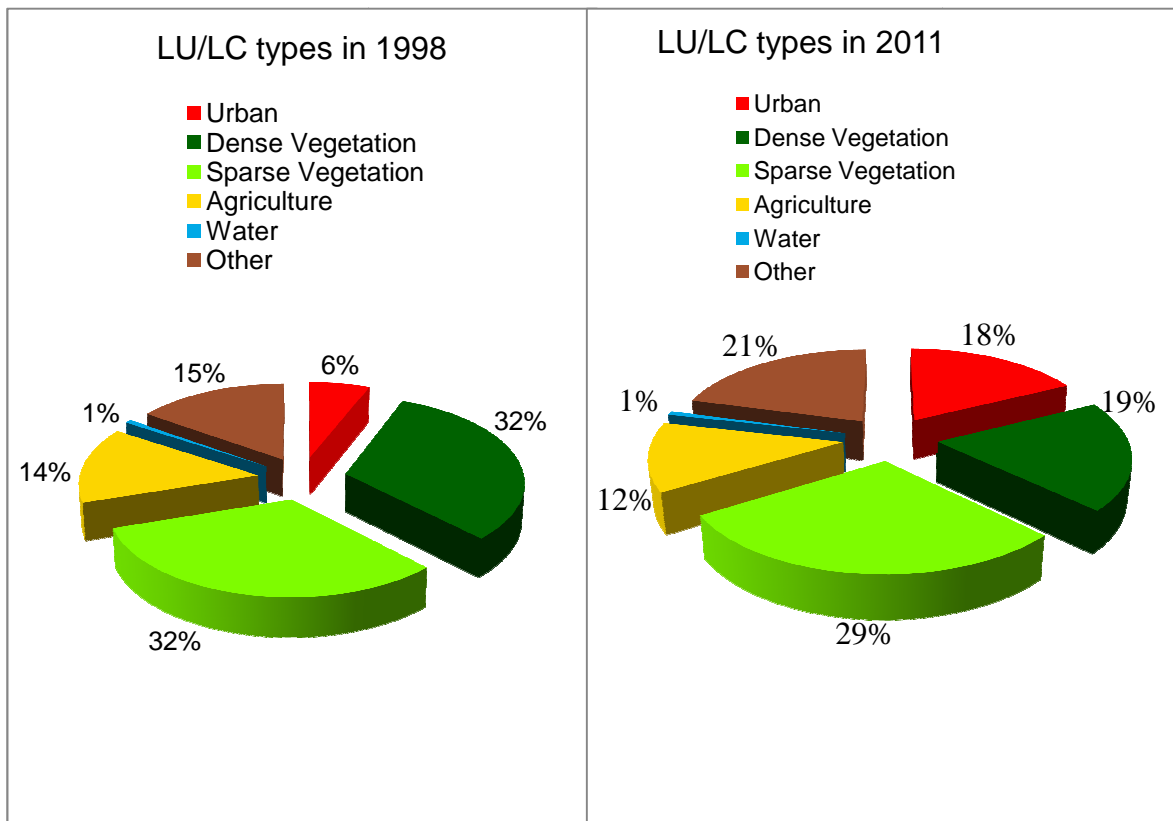
Figure 4.2 Changes in LU/LC classes in percentage between 1998 and 2011.
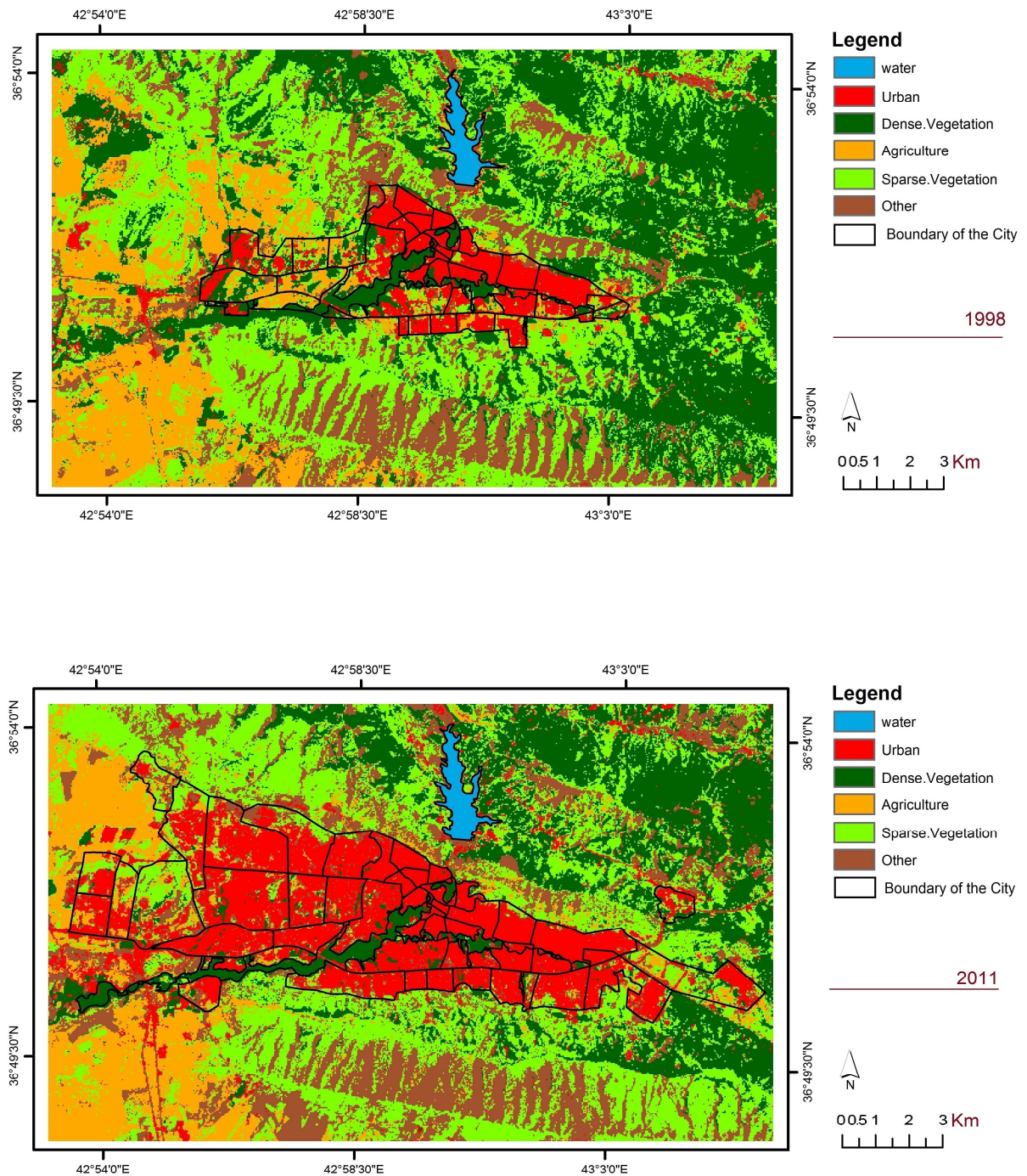
Figure 4.1 LU/LC maps of the Duhok city of years 1998 and 2011.

4.1.1. Classification accuracy assessment

Assessment of accuracy is a necessary step after each classification process. In this case, the error matrix technique was used which are the most widely used methods. After taking samples 240 random points (as shown in Figure (4.3)   and following all

classification stages, an accuracy assessment was obtained. Table (4.2) shows the results of this assessment. As we can see the overall accuracy of the classified image in 1998 is about (93%) with a kappa (0.91). On the other hand, the overall accuracy for the classified image in 2011 is (91%) with a kappa (0.88).

Table.4.2 Classification accuracy for years 1998 and 2011

The result of error matrix in 1998

	Urban	Dense vegetation	Sparse vegetation	Agriculture	Water	Other	Line total	Producer's accuracy (%)	User's accuracy (%)
Urban	42	0	0	0	0	0	42	77.78	100.00
Dense vegetation	1	53	3	1	0	1	59	95.83	92.00
Sparse vegetation	1	2	52	1	0	1	57	94.29	92.96
Agriculture	2	0	1	36	0	1	40	94.74	90.00
Water	0	0	0	0	3	0	3	100.00	100.00
Other	0	1	0	0	0	38	39	92.68	97.44
Top raw	18	72	70	38	1	41	240		

Classification accuracy = 93.33 %

Kappa statistics = 0.9124

The result of error matrix in 2011

	Urban	Dense vegetation	Sparse vegetation	Agriculture	Water	Other	Line total	Producer's accuracy (%)	User's accuracy (%)
Urban	51	0	0	1	0	4	56	98.08	91.07
Dense vegetation	0	45	0	0	0	0	45	88.24	100.00
Sparse vegetation	0	6	41	1	0	4	52	95.08	84.06
Agriculture	0	0	2	44	0	0	46	90.00	93.10
Water	1	0	1	0	1	0	3	100.00	100.00
Other	0	0	0	1	0	37	38	82.22	92.50
Top raw	52	51	61	30	1	45	240		

Classification accuracy = 91.25 %
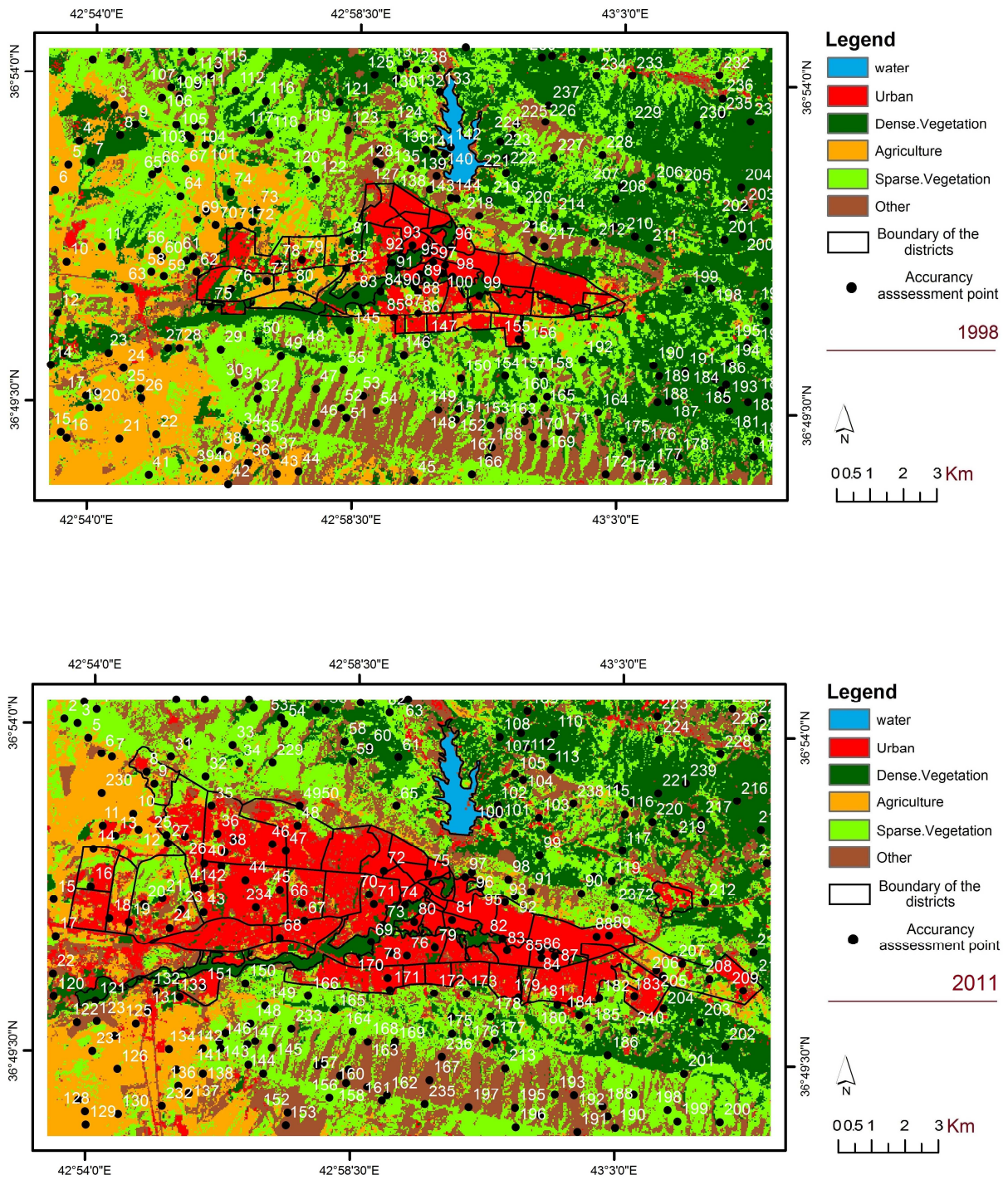
Kappa statistics = 0.8893

Figure 4.3 Classification accuracy maps for the years 1998 and 2011.

4.2. Change Detection Analysis

4.2.1. Change between 1998 and 2011

In remote sensing technology, change discovering is a vital application. It is a technology that ascertains any changes in specific characteristics within a period of time. It gives the spatial division of characteristics and qualitative and quantitative instruction with regard to feature changes. The quantitative analysis and the identification of the features and procedures of surface change is carried through from the unlike time of remote sensing data. It includes the type, division and quantity of any changes in terms of surfacing of ground type, boundary changes and trends after and before such changes. The analysis of change detection in this study has been performed in 1998 and 2011. The spatial division of changes is shown in Figure (4.4). As it is shown in table (4.3), the outcomes indicate that there is a rising trend towards the areas of urban at the expenditure of sparse vegetation, other and agriculture classes. On the other hand, there is a rising trend towards agricultural areas at the expenditure of sparse vegetation, other and urban. This change in urban to another class is due to population migration to urban areas spatially between 1998 and 2011 as shown in the table below, where the gray color represents no change.

Table 4.3 Change detection between1998-2011.

2011LULC (ha)	1998LULC(ha)						
	Urban	Dense Vegetation	Sparse Vegetation	Agriculture	Water	Other	Class Total
Urban	1054.53	29.25	16.38	12.51	0	100.26	1212.93
Dense veg.	623.52	3202.74	1488.33	386.28	0	711	6411.87
Sparse veg.	765.99	611.73	3349.17	636.48	0	1173.96	5159.61
Agriculture	814.77	54.63	321.03	1283.58	0	418.59	2892.6
Water	0	0.36	0	0	131.4	3.78	135.54
Other	310.77	70.92	705.24	174.78	7.92	1798.2	3067.83
Class total	3569.58	3969.63	5880.15	2493.63	139.32	4205.79	------------
Class change	2515.05	766.89	2530.98	1210.05	7.92	2407.59	------------
Image difference	-2356.6	2442.24	-720.54	398.97	-3.78	-1.137.96	------------

Legend

☐	Nochanged	■	Agriculture to Urban
■	Urban to Other	■	Agriculture to Sparse Veg.
■	Dense Veg. to Urban	■	Agriculture to Other
■	Dense Veg. to Sparse Veg.	■	Other to Urban
■	Dense Veg. to Agriculture	■	Other to Dense Veg.
■	Dense Veg. to Other	■	Othe to Sparse Veg.
■	Sparse Veg. to Urban	■	Other to Agriculture
■	Sparse Veg. to Dense Veg.	☐	Boundary of the city in 1998
■	Sparse Veg. to Agriculture	☐	Boundary of the city in 2011
■	Sparse Veg. to Other		

0 0.5 1   2   3 Km

N

Figure 4.4 Change detection map between (1998-2011).

4.3. Land Surface Temperature Retrieval

In this study a Radiative Transfer Equation (RTE) was employed to map out the spatial variation of LST for 1998 and 2011. The method was integrated with GIS techniques to allow a numerical and geographical analysis of the spatial and temporal distribution of LST. LST analyses were conducted with regard to the images for 1998 and 2011. The spatial and temporal variations of LST between these two years were mapped out, and can be seen in sequential colour in degrees centigrade represented in (4.5).

Figure 4.5 Land surface temperature for 1998 and 2011.
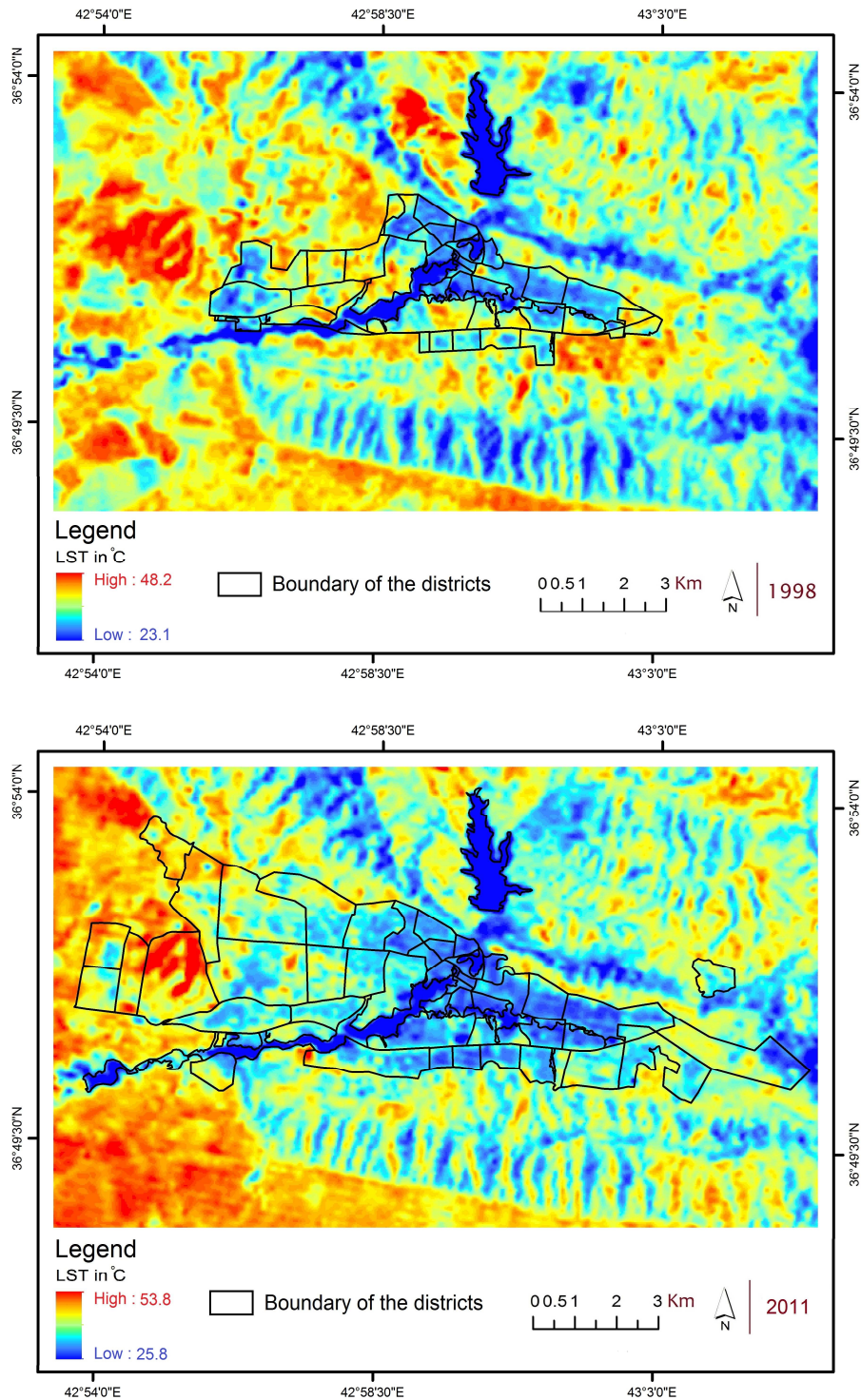
It is apparent from the results shown in Figure (4.5) that the hottest places in terms of surface temperature are concentrated outside the city for both years, while it is cooler inside the city and over the different classes of vegetation and the body of water as well. Therefore, the LST results of this study may not agree with the wider literature on LST and

urban areas which state that the LST in urban areas is higher than in surrounding areas. We can say this because according to our result, in Duhok the LST inside the city was lower than in the surrounding areas for both years taken in this study. This result in agreement with ((Ahmed *et al*. (2005), Kwarten and Small (2005), Habib (2007),Bounoua *et al*. (2009),. On the other hand, another significant result revealed by this study is that the maximum LST increased by 5º C for the total area, from 48ºC in 1998 to 53ºC in 2011, and the minimum LST increased by 2ºC from 23º C in 1998 to 25ºC in 2011. These changes in maximum and minimum LST, result from a number of factors. Firstly, there is the difference in time when the images were captured. This may have a role to play because the image for 1998 was captured on 13-06-1988 at (10:22:39 AM) and for 2011 it was captured on 17-06-2011 at (10:34:05 AM). The difference between the images is about 12 min in the morning which may have an effect on the difference in LST as well. On the other hand, the second reason is that the whole region faced serious environmental problems such as drought and desertification over the period of time under investigation. As weather station data shows, the mean temperature has increased and the mean precipitation has decreased since the 1990s. In addition, the report prepared by the IAU, UNEP, WHO, UNESCO, UNICEF, FAO and the Ministry of Environment in Iraq about climate change in Iraq (2012) shows that around 40,000 hectares are lost every year in the whole of Iraq due to climate change. The last factor relates to the decrease in vegetation classes in this area. In this study we classified the vegetation area into three different groups (dense, separated and agriculture); all of these classes decreased form 78.23 in 1998 to 60.93 in 2011. This reduction in vegetation classes led to reduced humidity and a decrease in the transpiration cooling effect of plants. In addition, the increasing of maximum LST from 48 to 53 may be due to an error in technique relating to pixels. This is because the LST temperature retrieved by satellite images depends on pixel reflectance. Therefore, higher pixel reflectance records higher LST. In this case we would expect that there were some areas in this region under construction when the images were captured, resulting in the high reflectance recorded in some pixels.

4.4. Spatial Distribution of Land Surface Temperatures in Dhuok City

Retrieving the LST in an urban area strongly depends on the surface energy balance (Voogt and Oke, 2003). On the other hand, the surface energy balance is measured based on the thermal characteristics of different surface features (Cartland, 2008) (as cited in Abdullah,2012). As a result, the variation in the distribution of LST within an urban area

may be identified by the nature of the materials that have been used to construct buildings, such as asphalt, concrete, rock and mud, and by differences in terms of land cover types such as buildings, green areas, water, and so on.

In order to investigate the spatial distribution of LST, and to identify the major hot and cool parts of the city in terms of LST, GIS techniques were used. The results of the spatial distribution of the LST in Duhok city are explained in the following section.

4.4.1. Spatial distribution of Land Surface Temperatures in 1998

The results of the spatial distribution of LST for 1998 reveals that the spatial LST pattern was non-equal and non-concentric (see Figure (4.6) and Table (4.4)).In general, the highest temperatures were recorded in the districts which were located around the city, and relatively remote from the old districts in Central Duhok. For example, Bahdinan, Botan, Shake, Nzarke, Peshasazi, Shandokha, Bntika, Peshangaha, Mhabad, L.malta, Sarbasti, Se grka, Ronhai,U.Malta and Azdai were identified as having the hottest surface temperatures (35,35,35,35,35,34,34,34,34,34,34,33,33,33,33 and 33ºC respectively). This was due to the fact that they had a lot of open areas or hard surfaces with no covering. In addition, it is important to note that other hot places were found in the districts of Peshaszy and Nizarke, both of which have an LST of 35ºC.This was due to their having buildings with aluminum roofs and bare areas which emit thermal energy due to human activities associated with the factory work in these areas. Furthermore, the districts which were newly built during this period have a higher surface temperature compared with older districts. For instance, Shahidan, Barushke and Bashur, which were new districts built in 1998, have an LST of 31ºC. This is higher than the districts which have existed for longer such as Khabat, Nuharda, Brayati, Gre Base, Dasnia, Shele and Kani Kshma where the mean LST was 29, 29, 29, 30,30,30 and 29ºC respectively.

 This difference is due to the fact that the older districts have slightly more green spaces which have existed for a long time, or there are no longer any open spaces which are not covered by anything. The opposite is true of the new districts, which have a lot of open spaces and a lack of green spaces. As a result, these new districts may absorb higher amounts of solar radiation while producing lower evaporation because of a lack of vegetation cover (Gartland, 2008) . In addition, it is well known that vegetation plays an important role in the process of retaining water within the ground. For this reason, land cover with a lack of vegetation cannot retain rainwater during the rainy season. As a

consequence, the land or the soil remains dry, and becomes warmer during the summer season when compared to vegetated areas (Abdullah,2012).

Table 4.4 give the following data: Mean LST in°C of main districts in Duhok City on 13-06-1998 at 10:22:39 AM and Mean LST in°C of main districts in Duhok City on 17-06-2011 at 10:34:05 .

No.	Name of Districts	Mean LST in °C 1998	Mean LST in °C 2011	No.	Name of Districts	Mean LST in °C 1998	Mean LST in °C 2011
1	Bahdinan	35	38	26	Gali	31	35
2	Botan	35	37	27	Shorsh	31	36
3	Shakhke	35	37	28	Bazar	31	35
4	Nzarke	35	38	29	Shahidan	31	34
5	Peshasazi	35	38	30	Baruske Bashur	31	30
6	Shandokha	34	38	31	Shele	30	34
7	Bin Tika	34	37	32	Dasnia	30	34
8	Peshangaha	34	37	33	Gre Base	30	35
9	Mhabad	34	35	34	Khabat	29	34
10	L.Malta	34	37	35	Nuhadra	29	34
11	Raza	33	36	36	Brayati	29	35
12	Sarbasti	33	36	37	Kani Khshma	29	35
13	Media	33	36	38	Veg. Dense	28	29
14	Mazi	33	37	39	water	25	26
15	Azadi	33	35	40	Kevla	-	42
16	Se Grka	33	34	41	Zrka	-	40
17	Ronahi	33	37	42	Zanko	-	43
18	U.Malta	33	38	43	Ailul u Gullan	-	41
19	Sarhaldan	33	35	34	Masika	-	41
20	Ashti	32	35	45	Tanahi	-	40
21	Nawroz	32	36	46	Avrusti	-	42
22	Dyari	32	32	47	Qasara	-	38
23	Barushke	32	30	48	Besre	-	41
24	Gafrke	31	37	49	Masika Roshava	-	42
25	K- Mhamadke	31	33	50	Etite	-	41
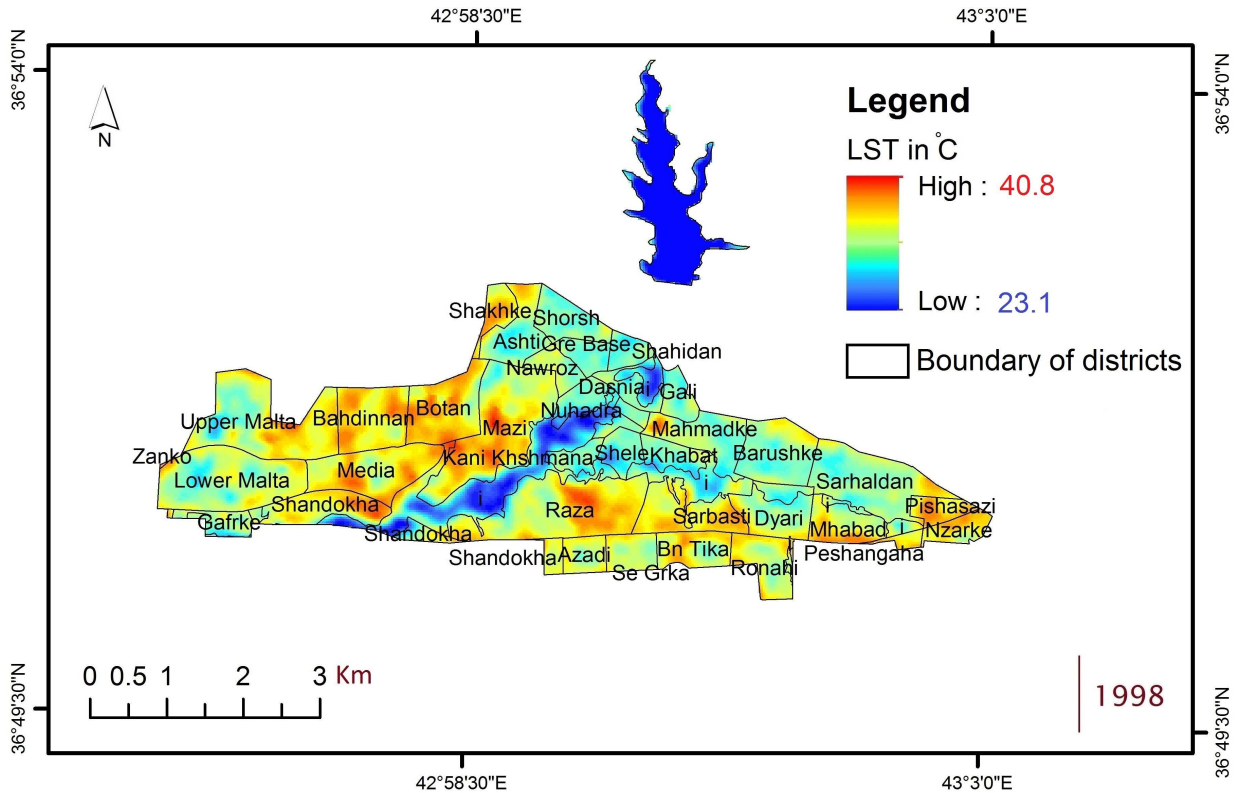
Figure 4.6 Spatial distribution of LST in the main districts of Duhok City on 13-06-1998 at 10:22:39 AM

4.4.2. Spatial distribution of Land Surface Temperatures in 2011

In 2011, the results reveal that the spatial pattern of LST were non-equal and non-concentric with regard to the districts, with slight changes in LST due to the fast and vast expansion of the city as shown in Figure (4.7) and Table (4.4). It seems that the mean LST in 2011 was higher than that in 1998 in almost all districts. Furthermore, the results in terms of the spatial distribution of LST in 2011 totally matched the results in 1998 in terms of the newly built districts, usually recording the hottest surface temperatures compared with the older districts. For instance in Kevla, Zrka, Zanko, Ail u Gulan, Masika, Tanahi, Avrusti, Besre, Masika Roshava, Etite and Qasara, the temperatures were 42, 40, 43, 41, 41, 40, 42, 41, 42, 41and 38ºC respectively. On the other, the district of Zanko recorded a high LST in this year due to the nature of this district which is almost without vegetation and hence leads the areas in terms of becoming warmer during the summer season when compared to vegetated areas. If we consider Figure (4.7), we can see the differences in spatial distribution in terms of surface temperature.

Therefore the results of the LST spatial distribution demonstrate that there is an observable variation among the districts in this city in terms of LST. In addition, the images were captured at the beginning of the summer. At this time of year, the ratio of sunlight observed on the ground surface increases as a result of clear skies, the vertical situation of sunlight according to the earth's surface and an obvious reduction of humidity in the air and the soil, all of which leads to recording a high surface temperature.
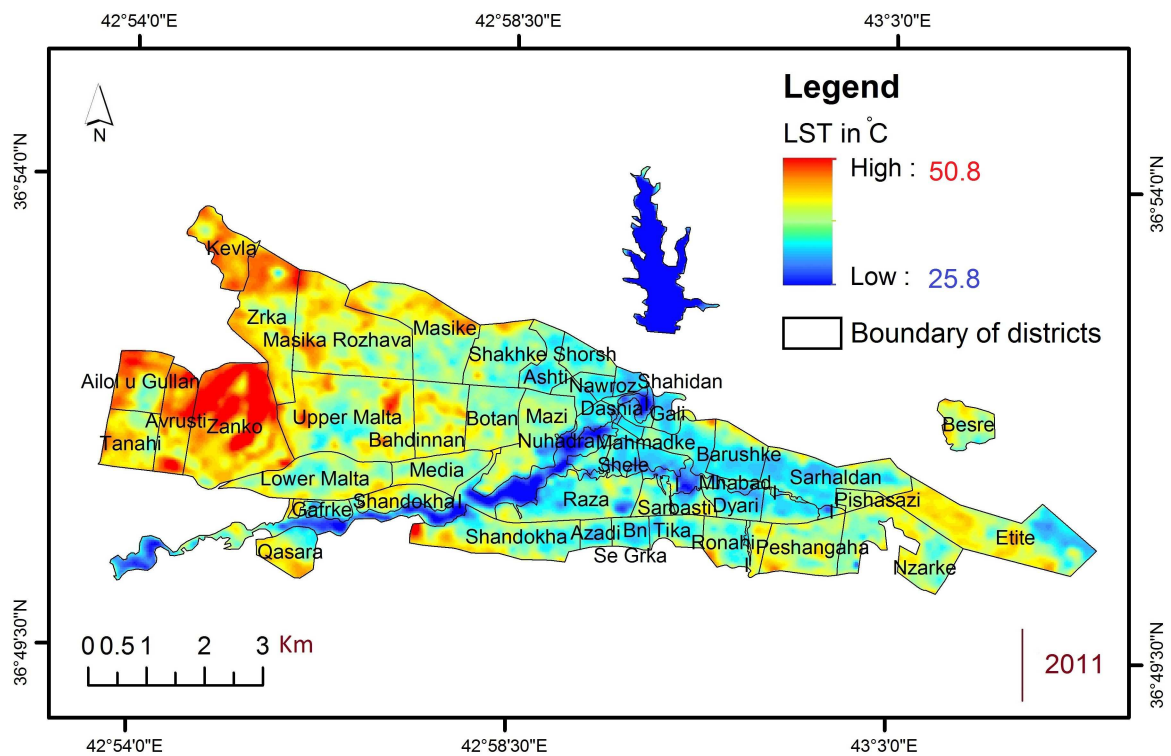
Figure 4.7 Spatial distribution of LST in the main districts of Duhok City on 17- 06-2011 at 10:34:05 AM .

In contrast, further investigation was employed to analyse the impact of urban expansion on LST during this period of time. As it appears from Table (4.4) , around 11 new districts were built between 1998 and 2011. For this reason, GIS techniques and data were used to detect the changes derived from the LST maps (see Figure (4.8)). The results revealed that the expansion of the city over the dry lands surrounding the city led to a decrease in LST of around 2ºC in some newly built districts as can be seen from the blue colour on the map, while the red colour refers to an increase in LST of more than 2ºC. Thus, the expansion of Duhok City over the other land cover in this region has led to a control and reduction of LST. This result totally matches that of other studies which were

done in nearly similar geographical situations such as the studies by Habib (2007), Kwarten and Small (2005) and Frey *et al*. (2005) in which they pointed out that constructing buildings over dry and desert land is a way to control the increase in LST and produce urban cool islands (UCI).
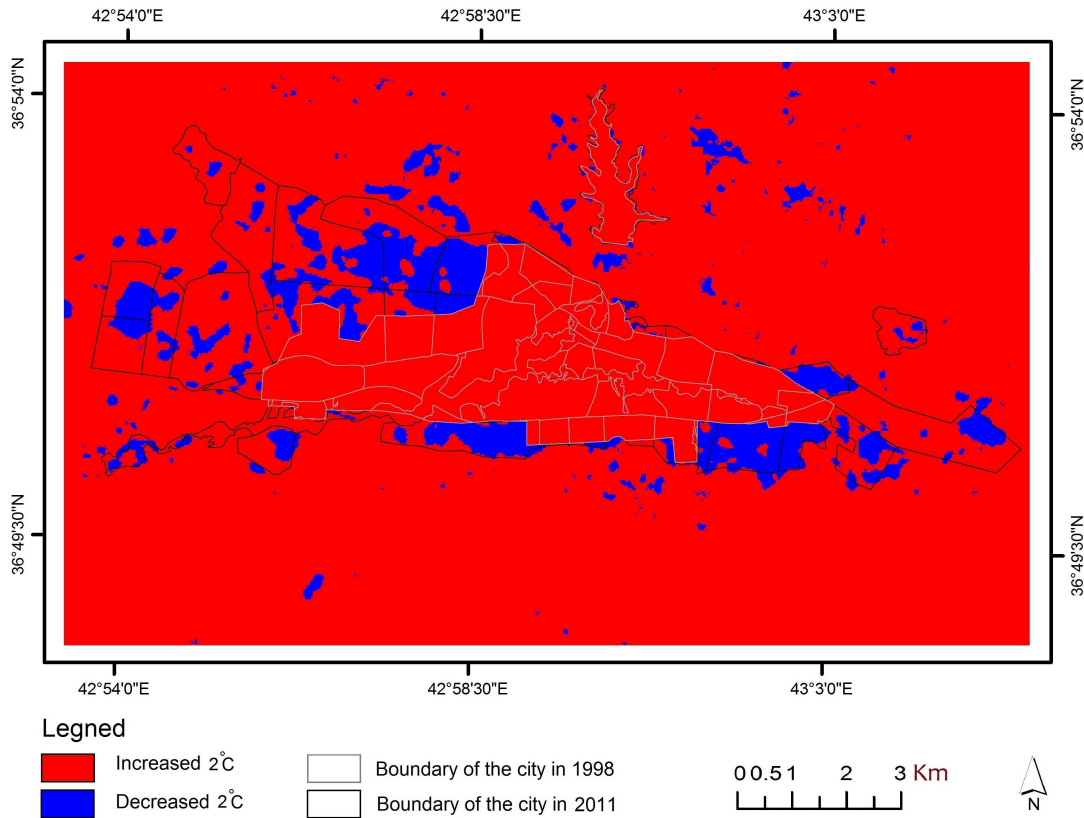
Figure 4.8 The change detection map based on LST for 1998 and 2011.

4.5. Relationship Between Land Surface Temperature and Different Land Use and Land Covers

The variation of LST depends on certain factors which have a great impact on the process of heating ground surfaces, such as soil moisture, land surface emissivity, albedo, vegetation abundance, and so on (Weng *et al*., 2004). Thus, each type of land cover has a particular characteristic which determines its LST.

For this reason, to find out the connection between different land covers and LST, the classified images and LST maps were imported into the ArcGIS software, in order to associate each class with the value of the LST as explained in Figure (3.9). This process has led to the extraction of a mean LST for each land cover type. This is an essential step

47

in terms of understanding the characteristics of the thermal signatures of each land cover class identified in this study. From the (4.9) it would appear that the lowest temperatures were recorded over a body of water (the Duhok Dam). This was 25ºC in 1998, and 28ºC in 2011. In addition, dense and sparse vegetation classes recorded low temperatures compared with other classes. The dense class recorded 30 ºC in 1998 and 32 ºC in 2011, while sparse classes recorded 31 ºC in 1998 and 34 ºC in 2011. It's important to note that, in general, the LST over all the above-mentioned classes saw an increase in temperature due to changes in the climatic and environmental factors as mentioned before.

In terms of urban land, temperatures of 37ºC and 40ºC in 1998 and 2011 were recorded respectively. In contrast, the highest temperature was recorded over the other classes - 39 ºC in 1998 and 42 ºC in 2011. The results of these high LSTs can be identified by, first: the other classes were classified based on unknown features on the images due to the low resolution of the Landsat images. Therefore, in most cases, the 'other class' consisted of barren land which usually records a high LST due to the lack of vegetation to protect the land from the heat of the sun, and any transpiration cooling due to the existence of plant life (Weng *et al*., 2004). As a result, this leads to lower humidity and leads to the land absorbing the heat of the sun directly, causing such land to become warmer more quickly than other land cover types. On the other hand, regarding other land cover classes such as the structures and materials which are used to construct artifacts in urban areas such as concrete, roads, buildings…. etc., they tend to absorb heat from the sun more slowly, and they also emit it more slowly. In other words, the absorbed heat in urban area tends to remain longer than in other land cover classes, and hard surfaces such as barren land do not hold heat for longer than urban land.

In general, in this study, urban land appears cooler than barren land due to the time of day at which the Landsat TM images were captured. Since this was the morning, the heating of the surface by the sun had just started and, as mentioned before, materials and structures used in urban areas usually become warmer more slowly and also become cooler more slowly than other land covers. For this reason, other and open classes recorded the highest LST compared to urban land cover(Abdullah,2012).
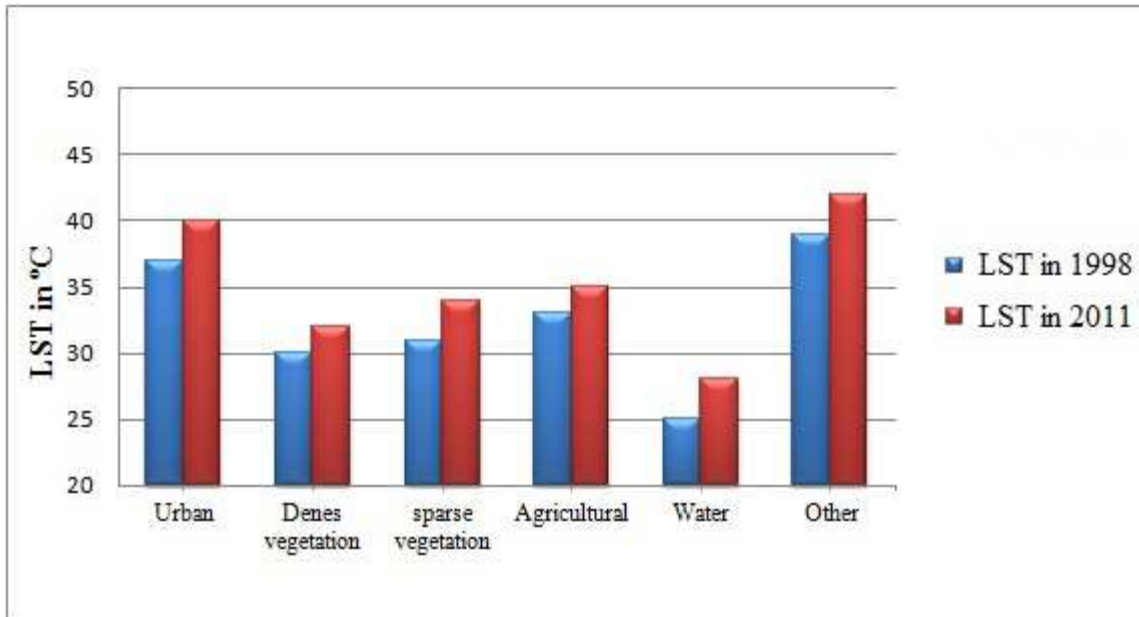
Figure 4.9 Mean LST for different LU/LC classes in 1998 and 2011.

4.6.Relationship Between Land Surface Temperature and the Normalized Different Vegetation Index

In the above section the difference in LST in terms of the different land cover classes was presented. However, according to the literature such as that of Kumar *et al*. (2012), Saleh (2011), Bounoua *et al*. (2009), Habib (2007), Ahmed *et al*. (2005) and Honjo *et al*. (2004), highly focused to find out the impact of vegetation on LST. This is because vegetation is widely identified as an important indicator of the control and reduction of LST. Thus, one of the most common vegetation indices was used in the form of NDVI. In general, the use of NDVI is widely documented in the literature to explore the relationship between LST and vegetation because it's a proper indicator for use when studying LST, and (Gallo *et al*., 1993).

Results of the NDVI maps were normalized between -1<=NDVI<=1. The negative value is indicative of water and other non-vegetated, non-reflective surfaces, while positive values stand for vegetated or reflective surfaces. Figure (4.10) shows the NDVI map for the study area for both years under consideration.

The results in terms of extracting NDVI reveal that there is a noticeable change in vegetation cover. It appears from the classified images that the all-vegetation cover (dense, sparse and agriculture) together decreased from 78.23 in 1998 to 60.93 in 2011. On the

49

other hand, the highest NDVI values were noted in green spaces, and the lowest were in barren land, urban land and on the body of water in the study area (Duhok Dam).
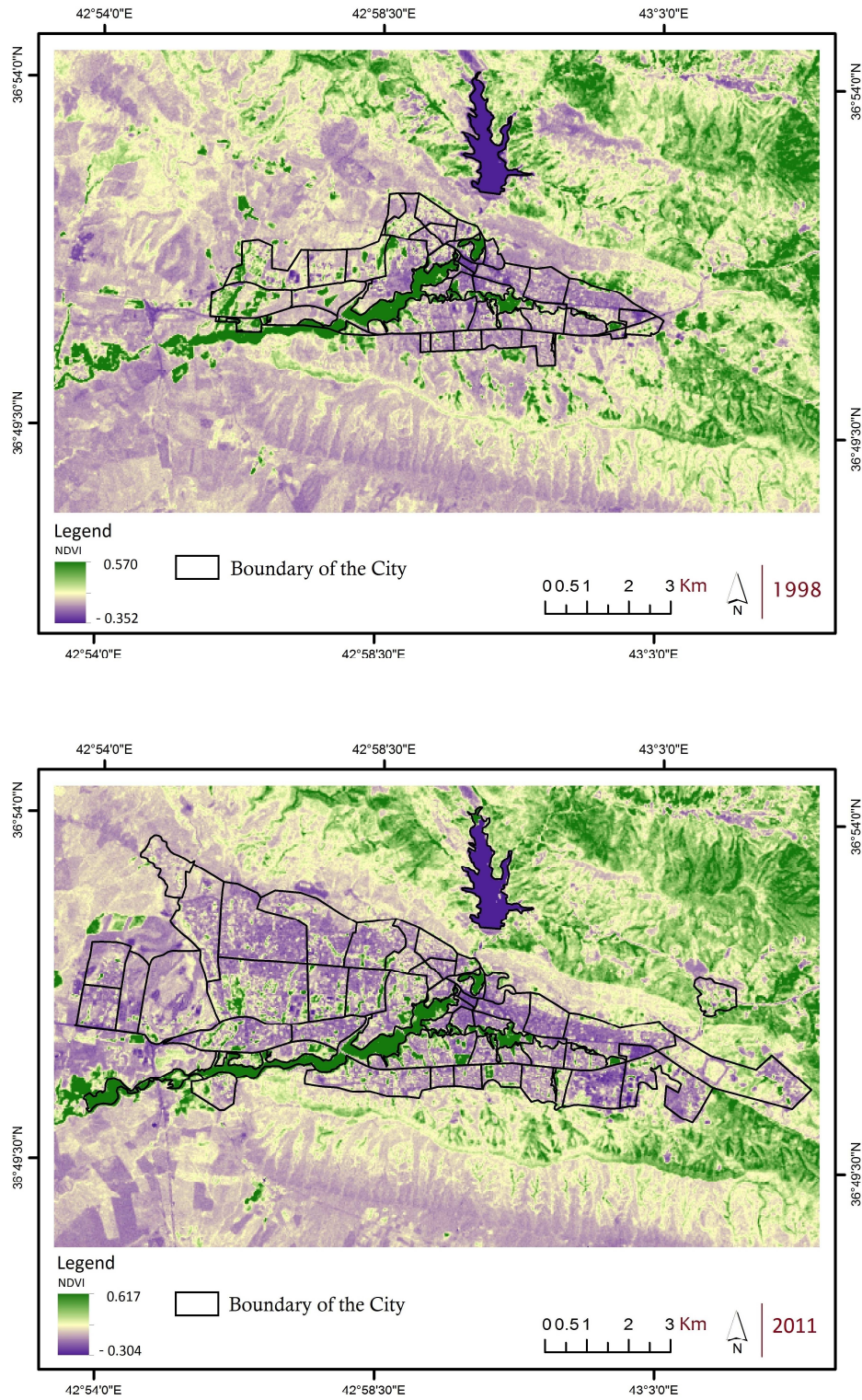
Figure 4.10 NDVI maps for 1998 and 2011.

Therefore, to find out the real relationship between LST and vegetation, Pearson's correlation coefficient analysis, as well as linear regression analysis, was used to evaluate the connection between LST and NDVI. Both were used because the use of correlation analysis alone cannot offer the correlation between variables and their degree of correlation (Saleh, 2011) (see Figures (4.11) and (4.12)). Thus, 40 random points were collected, using the same coordinates for LST and NDVI for each image separately (see Tables (4.5) and (4.6)).

The results of the Pearson correlation coefficient indicate that there is a strong negative correlation between LST and NDVI. For instance, the correlation result for 1998 is -0.86, and for 2011 it is -0.82. Therefore, this widely agrees with the literature, as various authors revealed negative correlations between LST and NDVI suck as studies by Kumar *et al*. (2012), Saleh (2011), Bounoua *et al*. (2009), Habib (2007), Ahmed *et al*. (2005) and Honjo *et al*. (2004).Furthermore, in order to evaluate to what extent NDVI values are able to predict changes in LST, the R squared value was extracted and found to be 0.734 in 1998 and 0.670 in 2011. These are reasonable values which show that NDVI is an important indicator when it comes to predicting changes in LST. In other words, vegetation is important when it comes to controlling LST as we found in this study due to the strong negative correlation between NDVI and LST. This means that by increasing NDVI values, the LST will decrease and the opposite is correct.

Table 4.5 Collected values from NDVI and LST maps for 1998

No.	NDVI	LST	No.	NDVI	LST
1	0.501	23	21	0.079	32
2	0.102	35	22	0.031	42
3	0.013	44	23	0.502	24
4	0.111	33	24	0.069	32
5	0.099	37	25	0.085	35
6	0.449	29	26	-0.076	46
7	0.201	31	27	0.063	37
8	0.052	39	28	0.138	30
9	-0.096	43	29	0.006	44
10	0.096	38	30	0.000	41
11	0.006	35	31	0.034	39
12	0.039	43	32	0.117	35
13	-0.009	48	33	0.027	41
14	0.199	30	34	0.106	34
15	0.104	36	35	0.076	39
16	0.034	37	36	0.405	27
17	-0.020	42	37	0.051	41
18	0.046	39	38	0.456	28
19	0.011	40	39	0.030	44
20	0.027	41	40	0.180	30

Table 4.6 Collected values from NDVI and LST maps for 2011

| No.	NDVI	LST	No.	NDVI	LST
1	-0.005	48	21	0.136	37
2	-0.006	47	22	0.090	36
3	0.069	44	23	0.498	28
4	0.017	42	24	0.190	32
5	0.009	40	25	0.030	39
6	-0.011	48	26	0.042	36
7	0.153	35	27	0.043	39
8	-0.027	39	28	-0.041	45
9	0.037	38	29	0.053	42
10	0.420	29	30	-0.002	50
11	0.034	40	31	0.136	36
12	0.111	36	32	-0.011	49
13	0.236	31	33	0.006	41
14	0.183	33	34	-0.071	42
15	0.115	35	35	0.106	39
16	0.409	26	36	-0.012	48
17	0.096	37	37	0.186	35
18	0.047	43	38	0.501	25
19	-0.009	46	39	0.000	38
20	0.069	31	40	0.068	47
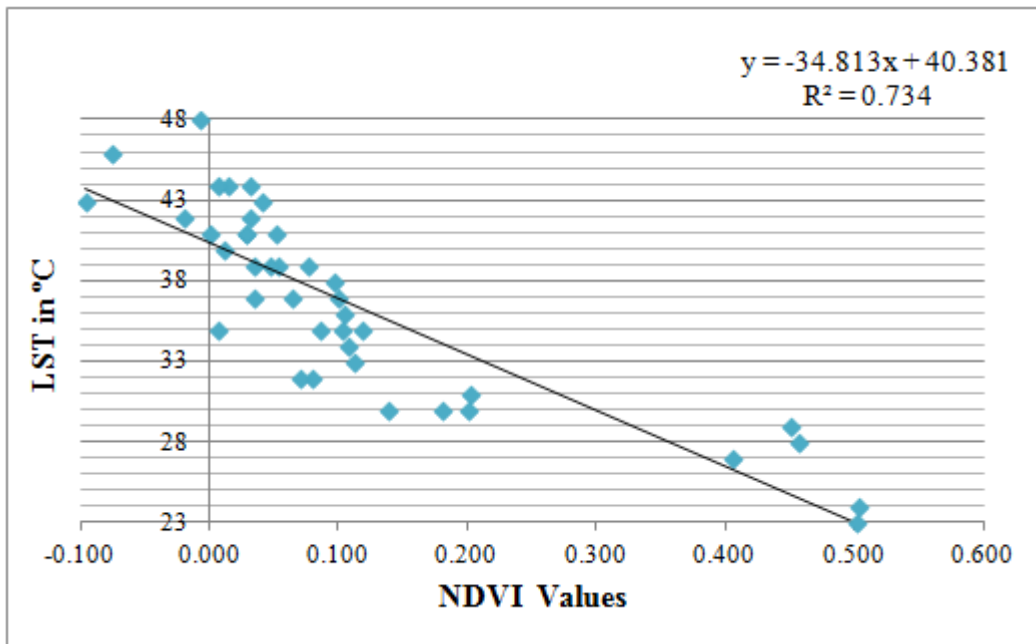
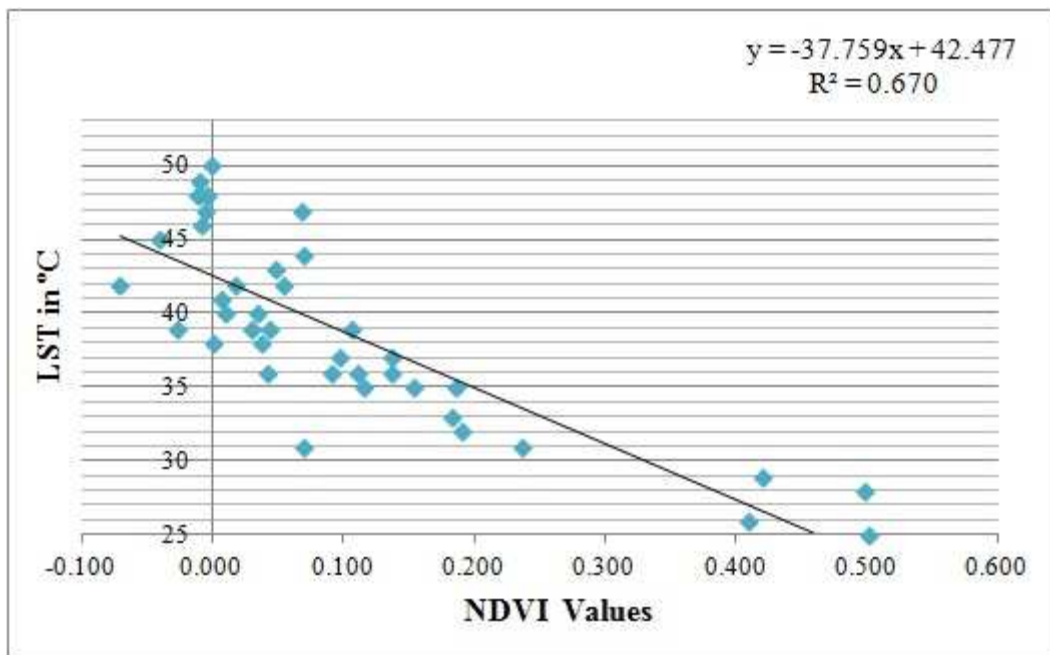Figure 4.11 Results of linear regression analysis of LST vs. NDVI for 1998.

Figure 4.12 Results of linear regression analysis of LST vs. NDVI for 2011.

5. CONCLUSION

This study had attempted to evaluate the impact of urban expansion in Duhok city on Land surface temperature between the years (1998 and 2011). Remote sensing techniques as well as GIS were used to achieve the main goals of this research. Landsat-5 TM data was used to classify different land covers and to retrieve LST for the study area for 1998 and 2011. has been categorized into six different classes as follows urban, dense vegetation, sparse vegetation, agriculture, water and other land. At the same time, with this classification, LST was retrieved for both years based on using the Landsat thermal band, while Radiative Transfer Equation(RTE) was used to convert digital data to LST. The results of the land cover classification revealed a remarkable expansion of urban areas over this period of time, while other forms of land cover decreased. In addition, the result of retrieving the LST shows that it had various forms from 1998 to 2011. In general, LST was increased due to environmental changes which led to the emergence of the drought phenomenon and led to decrease in vegetation cover.

In terms of the impact of urban expansion on LST, this study clearly underlines that Generally, the expansion of urbanisation has led to the control and in somehow decrease LST instead of having a negative impact. This result is because the region entirely changed from being a semi-desert during the June. However, the drawbacks of the expansion of Duhok city during this period of time can be identified in terms of natural and physical land cover changes, such as altering the vegetation cover to man-made land cover and so on.

On the other hand, data on the spatial distribution of LST based on the city districts was retrieved, and revealed a remarkable result in that the districts located around the city, or the newly built districts, recorded the highest LST for both years due to the lack of green spaces and to the existence of more open and surfaces in these districts. As a result, the open and surfaces noticed more heat during and generated more heat at night, hence during the day became warmer and faster than other land cover forms. Further investigation was undertaken so as to establish the connection between various earth covers and LST. As a result, barren land and urban land were identified as having the hottest surface temperatures for both years.

In contrast, vegetation and water bodies recorded the lowest LST among all of the present land covers in this regionn. As is shown clearly, there is a cooling effect on the LST of areas of greenery inside Dhuok city and its around areas. For this reason, this study selected vegetation and water as being important indicators with regard to the decrease and control of LST in this region. Further investigation was undertaken to validate the impact of vegetation on LST. This resulted in correlation and linear regression analyses between NDVI and LST values The analyses show that the strong correlation between NDVI and LST is negative.

Additionally, this study supported the idea that it is possible for the expanding built-up areas to have a positive role when it comes to controlling LST in a semi-arid or semi-desert environment, such as is clearly stated in the work of Habib (2007), Kwarteng & Small (2005) and Frey *et al*. (2005).

To sum up, the methods that were used in this study are highly efficient in terms of achieving the research objectives and answering the research questions in a scientific manner. In addition, this project shows the importance of using Landsat thermal band imaging integrated with GIS techniques. This approach plays a major role in urban environmental issues. It also acts as an effective tool when it comes to helping interested parties and urban planners to find solutions for problems arising from environmental changes.

REFERENCES

Anderson, J. R. 1976. A land use and Land Cover Classification System for use with Remote Sensor Data (Vol. 964). US Government Printing Office.

Armenakis, C., Leduc, F., Cyr, I., Savopol, F., & Cavayas, F. 2003. A Comparative Analysis of Scanned Maps and Imagery for Mapping Applications.ISPRS *Journal of Photogrammetry and Remote Sensing*, 57(5), 304-314.

Arnfield, A. J. 2003. Two Decades of Urban Climate Research: a Review of Turbulence, Exchanges of Energy and Water, and the Urban Heat Island. *International Journal of Climatology*, 23(1), 1–26.

Ahmed, B.M., Hata, T., Tanakamaru, H., Abdelhadi, A.W. and Tada, A. 2005 'Spatial Analysis of Land Surface Temperature and Evapotranspiration for Some Land use/cover Types in the Gezira area, Sudan', Nogyo Doboku Gakkai Kyushu Shibu Koenshu, Vol. 86, pp. 264-265.

Akbari, H., Bell, R., Brazel, T., Cole, D., Estes, M., Heisler, G., … Zalph, B.2008. Reducing Urban Heat Islands : Compendium of Strategies Urban Heat Island Basics.

Barsi, J. A., Schott, J. R., Palluconi, F. D., & Hook, S. J. 2005 Validation of a Web-Based Atmospheric Correction Tool for Single Thermal Band Iinstruments. In *Optics & Photonics* 2005 (pp. 58820E-58820E). International Society for Optics and Photonics.

Bounoua, L., Safia, A., Masek, J., Peters-Lidard, C., & Imhoff, M. L. 2009. Impact of Urban Growth on Surface climate: A Case Study in Oran, *Algeria. Journal of applied meteorology and climatology*, 48(2), 217-231.

Bhatta, B. 2010. Analysis of Urban Growth and Sprawl from Remote Sensing Data. Springer Science & Business Media.

Crist, E. P., & Cicone, R. C. 1984. A Physically-Based Transformation of Thematic Mapper Data---The TM Tasseled Cap. Geoscience and Remote Sensing, IEEE Transactions On, (3), 256-263.

Chavez, P. S.1996.Image-Based Atmospheric Corrections-revisited and Improved. *Photogrammetric engineering and remote sensing*, 62(9), 1025-1035.

Chander, G., Helder, D. L., & Boncyk, W. C. 2002. Landsat-4/5 Band 6 Relative Radiometry. *Geosciences and Remote Sensing, IEEE Transactions on*,40(1), 206-210.

Chander, G., & Markham, B. 2003. Revised Landsat-5 TM Radiometric Calibration Procedures and Post Calibration Dynamic Ranges. *Geosciences and Remote Sensing, IEEE Transactions on*, 41(11), 2674-2677.

Congalton, R.G. and Green, K. 2009 Assessing the Accuracy of Remotely Sensed Data : Principles and Practices, 2nd Edition, New York: Taylor & Francis Group.

Chuvieco, E. and Huete, A.2010 Fundamental of Satellite Remote Sensing, New York: Taylor and Francis Group.

Campbell, J.B. and Wynne, R.H. 2011 Introduction to Remote Sensing, 5th Edition, New York: THE GUILFORD PRESS.

Foody, G. M., & Mathur, A.2004. Toward Intelligent training of Supervised Image Classifications: Directing Training Data Acquisition for SVM Classification. *Remote Sensing of Environment*, 93(1), 107-117.

Frey, C.M., Rigo, G. and Parlow, E. 2005 'The Cooling Effect of Cities in a Hot and Dry Environment', Global Developments in Environmental Earth Erbservation from Space. Proceedings of the 25th EARSeL Symposium, Porto, Portugal,pp. 169-174.

Gillespie, A., Rokugawa, S., Matsunaga, T., Cothern, J. S., Hook, S., & Kahle, A. B. 1998. A Temperature and Emissivity Separation Algorithm for Advanced Spaceborne Thermal Emission and Reflection Radiometer (ASTER) images.*Geoscience and Remote Sensing*, *IEEE Transactions on*, 36(4), 1113-1126.

Grimond, C. S. B.2005.Progress in Measuring and Observing the Urban Atmosphere. Theoretical and Applied Climatology, 84(1-3), 3–22.

Gartland, L.2008 Heat Islands: Understanding and Mitigating Heat in Urban Areas, London: Earth scan.

Gao, J.2009 Digital Analysis of Remotely Sensed Imagery, New York: McGraw - Hill Companies,Inc.

Huang, C., Wylie, B., Yang, L., Homer, C., & Zylstra, G. 2002. Derivation of a Tasseled Cap Transformation Based on Landsat 7 at-Satellite Reflectance. *International Journal of Remote Sensing*, 23(8), 1741-1748.

Honjo, T., Ueda, H., Nagatani, Y., Lim, E. and Umeki, K. 2004'Analysis of Surface Temperature of Urban Green Spaces by using LANDSAT TM and ETM+data', Environmental Information Science, pp. 259-264.

Healey, S. P., Cohen, W. B., Zhiqiang, Y., & Krankina, O. N. 2005. Comparison of Tasseled Cap-Based Landsat Data Structures for use in Forest Disturbance Detection. *Remote Sensing of Environment*, 97(3), 301-310.

H.J.Abdullah,2012 The Use of Landsat-5 TM Imagery to Detect Urban Expansion and Its Impact on Land Surface Temperatures in The City of Erbil, Iraqi Kurdistan Unpublished Master thesis, University of Leicester ,UK, Leicester.

Ifatimehin, O. O. 2007. An Assessment of Urban Heat Island of Lokoja Town and Surroundings Using Landsat ETM data. *FUTY Journal of the Environment*,2(1), 100-108.

Jin, M., & Dickinson, R. E.1999. Interpolation of Surface Radiative Temperature Measured from Polar Orbiting Satellites to a Diurnal cycle: 1. Without Clouds. *Journal of Geophysical Research: Atmospheres* (1984–2012),104(D2), 2105-2116.

Jiménez-Muñoz, J. C., & Sobrino, J. A. 2003. A Generalized Single-Channel Method for Retrieving Land Surface Temperature from Remote Rensing Data .*Journal of Geophysical Research: Atmospheres* (1984–2012), 108(D22).

Kwarteng, A. Y., & Small, C. 2005. Comparative Analysis of Thermal Environments in New York City and Kuwait City. Proceedings, *Remote Sensing of Urban Areas (URS 2005), Tempe, Arizona, USA, March*, 14-16.

Kerr, Y.H., Lagouarde, P.J., Nerry, F. and Ottle, C. 2005 'Land Surface Temperature Retrieval Techniques and Applications: Case of the AVHRR', in Quattrochi, D.A. and Luvall, J.C. (ed.) *Thermal Remote Sensing in Land Surface Processes, New York: CRC PRESS*.

Kiage, L. M., Liu, K. B., Walker, N. D., Lam, N., & Huh, O. K.2007. Recent Land Cover/use Change Associated with Land Degradation in the Lake Baringo Catchment, Kenya, East Africa: Evidence from Landsat TM and ETM+.*International Journal of Remote Sensing*, 28(19), 4285-4309.

Kumar, K. S., Bhaskar, P. U., & Padmakumari, K. 2012. Estimation of Land Surface Temperature to Study Urban Heat Island Effect using Landsat ETM+ Image. *International Journal of Engineering Science and Technology*, 4(2), 771-778.

Lillesand T.M., Kiefer R.W., 1994, Remote Sensing and Image Interpretation – A Textbook, 3rd Edition, Wiley. New York.

Levin, N. 1999 Fundamentals of Remote Sensing. [Online], Available: http://geography.huji.ac.il/personal/Noam%20Levin/1999-fundamentals-of-Remote-sensing.pdf [20 April 2012].

Lillesand, T.M., Kiefer, R.W. and Chipman, J.W. 2008 Remote Sensing and Image Interpretation, 6th edition, 111 River Street, Hoboken: NJ: John Wiley and Sons, Inc.

Markham B.L., Barker J.L., 1986, Landsat MSS and TM Post-Calibration Dynamic Ranges, Exoatmospheric Reflectances and At-Satellite Temperatures, Earth Observation Satellite Co., Lanham, MD, Landsat Tech. Note 1, Aug.

Mather, P.M. 2004 Computer Processing of Remotely-Sensed Images, 3rd Edition, Chichester: John Wiley & Sons, Ltd.

Mills, G. 2007. Luke Howard, Tim Oke and the Study of Urban Climates. Weather, 63, 153–157.

Mitsch, W.J. and J.G. Gosselink. 2007. Wetlands, 4th ed., John Wiley & Sons, Inc., New York, 582 pp.[3].

Mallick, J., Kant, Y., & Bharath, B. D. 2008. Estimation of Land Surface Temperature Over Delhi using Landsat-7 ETM+. *J Indian Geophys Union*, 12(3), 131-140.

Nichol, J. E. 1994. A GIS-based Approach to Microclimate Monitoring in Singapore's High-Rise Housing Estates. *Photogrammetric Engineering and Remote Sensing*, 60(10), 1225-1232.

Oke, T. R. 1988a. The Urban Energy Balance. Progress in Physical Geography, 12(4), 471–508.

Oluseyi, I. O., Danlami, M. S., & Olusegun, A. J. 2011. Managing Land Use Transformation and Land Surface Temperature Change in Anyigba Town, Kogi State, Nigeria. *Journal of Geography and Geology*, 3(1), p77.

Oguz, H. 2013. LST Calculator: a Program for Retrieving Land Surface Temperature from Landsat TM/ETM+ imagery .*Environmental Engineering and Management Journal*, 12(3), 549-555.

Prakash, A. 2000. Thermal Remote Sensing: Concepts, Issues and Applications. International Archives of Photogrammetric and Remote Sensing,33(B1; PART 1), 239-243.

Prigent, C., Aires, F., & Rossow, W. B. 2003. Land Surface Skin Temperatures from a Combined Analysis of Microwave and Infrared Satellite Observations for an all Weather Evaluation of the Differences Between air and Skin Temperatures. *Journal of Geophysical Research: Atmospheres* (1984–2012), 108(D10).

Qin, Z. H., Karnieli, A., & Berliner, P. 2001. A Mono-Window Algorithm for Retrieving Land Surface Temperature from Landsat TM Data and its Application to the Israel-Egypt Border Region. *International Journal of Remote Sensing*, 22(18), 3719-3746.

Rajeshwari, A., & Mani, N. D. Estimation of Land Surface Temperature of Dindigul district using Landsat 8 Data. International Journal of Research in Engineering and Technology, 3(05), 122-126.

Rizwan, A. M., Dennis, L. Y., & Chunho, L. I. U. 2008. A Review on the Generation, Determination and Mitigation of Urban Heat Island. *Journal of Environmental Sciences*, 20(1), 120-128.

Snyder, W. C., Wan, Z., Zhang, Y., & Feng, Y. Z. 1998. Classification-Based Emissivity for Land Surface Temperature Measurement from Space. *International Journal of Remote Sensing*, 19(14), 2753-2774.

Song, C., Woodcock, C. E., Seto, K. C., Lenney, M. P., & Macomber, S. A. 2001. Classification and Change Detection using Landsat TM data: When and How to Correct Atmospheric Effects?. *Remote sensing of Environment*, 75(2), 230-244.

Saleh, S. A. 2011. Impact of Urban Expansion on Surface Temperature in Baghdad, Iraq using remote sensing and GIS techniques. *Canadian Journal on Environmental, Construction and Civil Engineering*, 2(8), 193-202.

Sun, D., & Pinker, R. T. 2003. Estimation of Land Surface Temperature from a Geostationary Operational Environmental Satellite (GOES□8). *Journal of Geophysical Research: Atmospheres* (1984–2012), 108(D11).

Sobrino, J. A., Jimenez Munoz, J. C., & Paolini, L. 2004. Land Surface Temperature Retrieval from LANDSAT TM 5. Remote Sensing of Environment,90(4), 434-440.

Sobrino, J. A., Jiménez-Muñoz, J. C., Sòria, G., Romaguera, M., Guanter, L., Moreno, J., ... & Martinez, P. (2008). Land Surface Emissivity Retrieval from Different VNIR and TIR sensors. *IEEE Transactions on Geosciences and Remote Sensing*, 46(2), 316-327.

Skurikhin, A. N., Gangodagamage, C., Rowland, J. C., & Wilson, C. J. 2013. Arctic Tundra ice-wedge Landscape Characterization by Active Contours Without Edges and Structural analysis using High-Resolution Satellite Imagery. *Remote Sensing Letters*, 4(11), 1077-1086.

Singh, A., Singh, S., Garga, P. K., & Khanduri, K. 2013. Land Use and Land Cover Change Detection: A Comparative Approach Using Post Classification Change Matrix and Discriminate Function Change Detection Methodology of Allahabad City. *International Journal of Current Engineering and Technology*, ISSN, 2277-4106.

Thorne, K., Markharn, B., Barker, P. S., & Biggar, S. 1997. Radiometric Calibration of Landsat. *Photogrammetric Engineering & Remote Sensing*, 63(7), 853-858.

Tso, B. and Mather, P.M. 2009 Classification Methods For Remotely Sensed Data, 2nd Edition, New York: Taylor & Francis Group.

Valor, E., & Caselles, V. 1996. Mapping Land Surface Emissivity from NDVI: Application to European, African, and South American areas. *Remote sensing of Environment*, 57(3), 167-184.

Voogt, J. A., & Oke, T. R. 2003. Thermal Remote Sensing of Urban Climates. Remote sensing of environment, 86(3), 370-384.

Watson, K. 1992. Spectral Ratio Method for Measuring Emissivity. *Remote Sensing of Environment*, 42(2), 113-116.

Wan, Z., & Dozier, J. 1996. A Generalized Split-Window Algorithm for Retrieving Land-Surface Temperature from Space. *Geoscience and Remote Sensing, IEEE Transactions on*, 34(4), 892-905.

Weng, Q., Lu, D., & Schubring, J. 2004. Estimation of Land Surface Temperature–Vegetation Abundance Relationship for Urban Heat Island Studies .*Remote sensing of Environment*, 89(4), 467-483.

Zhang, J., Wang, Y., & Li, Y. 2006. A C++ Program for Retrieving Land Surface Temperature from the Data of Landsat TM/ETM+ Band6. Computers & Geosciences, 32(10), 1796-1805.

Zhang, Q., & Ban, Y. 2011. Evaluation of Urban Expansion and Its Impact on Surface Temperature in Beijing, China. In Urban Remote Sensing Event (JURSE), 2011 Joint (pp. 357-360). IEEE.

CURRICULUM VITAE

Personal information

Name	: Daban Kadhim Omar DABBAGH
Nationality	: Iraqi
Date and place of birth	: 26 April, 1987 Erbil, Iraq
Marital Status	: Single
Telephone	: (+964) 750 456 81 62
Email	: dabandabbagh@gmail.com
	: dabandabbagh@hotmail.com

Educational Background

Degree	Place of Education	Date of Graduate
Bachelor's Degree	Salahaddin University College of Arts Department of Geography	2008

Language Skills

Kurdish, English

Publications

Hakan Oğuz, Daban Kadhim Omar DABBAGH, 2015. Coğrafi Bilgi Sistemleri ve Uzaktan Algılama Teknikleri Kullanarak Kent Büyümesinin Yer Yüzey Sıcaklığı Üzerin Etkisinin Belirlenmesi: Duhok-IRAQ Örneği. Ecology Sempozyumu,Sinop.Pp 398.